View metadata, citation and similar papers at core.ac.uk

brought to you by CORE

provided by Dartmouth Digital Commons (Dartmouth College)

Dartmouth College
Dartmouth Digital Commons

Open Dartmouth: Faculty Open Access Articles

3-1-1983

Extreme Variability in the Be-Type, Periodic Recurrent X-Ray Transient A0538 - 66: A Highly Eccentric Interacting Binary

P. A. Charles
University of Oxford

L. Booth
University of Oxford

R. H. Densham
University of Oxford

G. T. Bath
University of Oxford

J. R. Thorstensen
Dartmouth College

Follow this and additional works at: https://digitalcommons.dartmouth.edu/facoa

Part of the Astrophysics and Astronomy Commons

Recommended Citation

Charles, P. A.; Booth, L.; Densham, R. H.; Bath, G. T.; and Thorstensen, J. R., "Extreme Variability in the Be-Type, Periodic Recurrent X-Ray Transient A0538 - 66: A Highly Eccentric Interacting Binary" (1983). *Open Dartmouth: Faculty Open Access Articles*. 1886.
https://digitalcommons.dartmouth.edu/facoa/1886

This Article is brought to you for free and open access by Dartmouth Digital Commons. It has been accepted for inclusion in Open Dartmouth: Faculty Open Access Articles by an authorized administrator of Dartmouth Digital Commons. For more information, please contact dartmouthdigitalcommons@groups.dartmouth.edu.

1983MNRAS.202..657C

Mon. Not. R. astr. Soc. (1983) **202**, 657–682

Extreme variability in the Be-type, periodic recurrent X-ray transient A0538 – 66: a highly eccentric interacting binary

P. A. Charles★, L. Booth, R. H. Densham and G. T. Bath
Department of Astrophysics, University of Oxford, South Parks Road, Oxford OX1 3RQ

J. R. Thorstensen★ *Department of Physics and Astronomy, Dartmouth College, Hanover, NH 03755, USA*

I. D. Howarth and A. J. Willis *Department of Physics and Astronomy, University College London, Gower Street, London WC1E 6BT*

G. K. Skinner *Department of Space Research, University of Birmingham, PO Box 363, Birmingham B15 2TT*

E. Olszewski★ *Department of Astronomy, University of Washington, Seattle, WA 98195, USA*

Received 1982 May 20; in original form 1982 March 15

Summary. We present optical spectroscopy and photometry and *IUE* spectroscopy of the counterpart of the extremely powerful LMC recurrent X-ray transient A0538 – 66. During one 16.6 day outburst cycle at the end of 1980 December the optical spectra show steadily increasing Balmer and He I emission (indicative of an expanding envelope) superposed on a B2 III–IV spectrum. There is a substantial optical brightness increase of 2 mag at the peak, accompanied by the sudden turn-on of He II λ4686. These and other optical spectra show significant radial velocity changes but we can find *no* clear correlation with the 16.6 day cycle. Further optical and *IUE* spectra were obtained at the peak of subsequent outbursts, and these show very strong and broad ($\sim 5000\,\mathrm{km\,s^{-1}}$) emission lines. We interpret the system as a $\sim 1\,M_\odot$ compact object in a highly eccentric ($e \sim 0.7$) orbit about the $\sim 12\,M_\odot$ B star with a binary period equal to the flare period. Continuum measurements indicate that the emitting region at outburst is several times the size of the B star thus implying that at periastron passage the envelope of the primary is tidally expanded by the neutron star. Although this is now the best example of a growing group of recurrent X-ray transients, A0538 – 66 is unique in its optical behaviour and peak L_x when compared with other galactic X-ray transients and shell/Be stars.

★Visiting Astronomers, Cerro Tololo Inter-American Observatory, operated by the Association of Universities for Research in Astronomy, under contract with the National Science Foundation.

Downloaded from https://academic.oup.com/mnras/article-abstract/202/3/657/967984
by Dartmouth College Library user
on 26 April 2018

© Royal Astronomical Society • Provided by the NASA Astrophysics Data System

1983MNRAS.202..657C

1 Introduction

The recurrent X-ray transient sources now represent a substantial class of galactic objects that are, by their very nature, difficult to study extensively. They can be divided into two groups on the basis of their optical primaries: the low-mass systems (e.g. Aql X-1 Thorstensen, Charles & Bowyer 1978) which are optically faint outside their outbursts; and those with high masses (e.g. A0535+26 Margon *et al.* 1977). It would clearly be of enormous observational and theoretical value to find an object which displayed the characteristics of transient X-ray sources (i.e. underwent major outbursts) on a short and predictable time-scale.

Ariel V observations of the LMC in 1977 led to the discovery by White & Carpenter (1978) of the periodic recurrent transient X-ray source A0538 – 66. Subsequent X-ray flares were observed with the *HEAO-1* Modulation Collimator which enabled Johnston, Griffiths & Ward (1980) to obtain a sufficiently precise position (~ 30 arcsec) that the source could be identified with a variable star. Skinner (1980, 1981) used *HEAO-1* Large Area Sky Survey data and archival plate material to show that the star flares simultaneously at X-ray *and* optical wavelengths (by ~ 2 mag) and that these flares recur with a period of 16.6 days. However, optical and X-ray observations throughout 1980 (Johnston *et al.* 1980; Pakull & Parmar 1981; Murdin, Branduardi-Raymont & Parmar 1981) revealed little activity and no outbursts.

This object is highly unusual for several reasons.

(i) The star is most likely to be in the LMC (see later) which implies $L_x \sim 10^{39}$ erg s^{-1} at outburst peak, which is ~ 10 times greater than *any other* galactic X-ray source and ~ 10 times greater than the Eddington luminosity for a $1 M_\odot$ compact object: it also has a high L_x/L_{opt} ($\gtrsim 1$ at peak) for an early-type system.

(ii) Optical spectroscopy of A0538 – 66 during quiescence is *broadly* consistent with that of a 'B-type star'. However, the range of optical variability is certainly *not* consistent with a normal early-type star.

(iii) At both optical and X-ray wavelengths, the star appears to undergo transitions between high and low activity on a time-scale of ~ 1 yr (Skinner *et al.* 1980; Pakull & Parmar 1981), which may be associated with a varying shell phase as is seen in galactic Be stars.

Spectroscopic and photometric monitoring at both optical and UV wavelengths was accomplished at CTIO, AAO and with *IUE* for much of a single outburst cycle in 1981 January together with scattered observations during subsequent outbursts. A preliminary presentation of some of these results was given by Charles *et al.* (1981, see also Charles & Thorstensen 1981). Here we give the fully analysed results and discuss models that might explain the extraordinary behaviour in this object.

2 Observations

A complete log of all the observations of A0538 – 66 reported here is presented in Table 1. Details of the individual observing runs (optical photometry, spectroscopy and UV spectroscopy) are given below.

2.1 CTIO (1980 December 27–1981 January 6)

We monitored A0538 – 66 photographically from December 27–29 with the CTIO Yale 1-m telescope, Carnegie image tube camera (S20) and filter matching closely the Johnson *B* band. Measurements on all three nights were consistent with the quiescent level of $B \sim 15$. Plate 1 is an enlargement of the A0538 – 66 region.

Downloaded from http://adsabs.harvard.edu/cgi-bin/nph-article_abstract?bibcode=1983MNRAS.202..657C
by Dartmouth College Library user
on 26 April 2018

© Royal Astronomical Society • Provided by the NASA Astrophysics Data System

Downloaded from https://academic.oup.com/mnras/article-abstract/202/3/657/967884
by Dartmouth College Library user
on 26 April 2018

© Royal Astronomical Society • Provided by the NASA Astrophysics Data System

1983MNRAS.202..657C

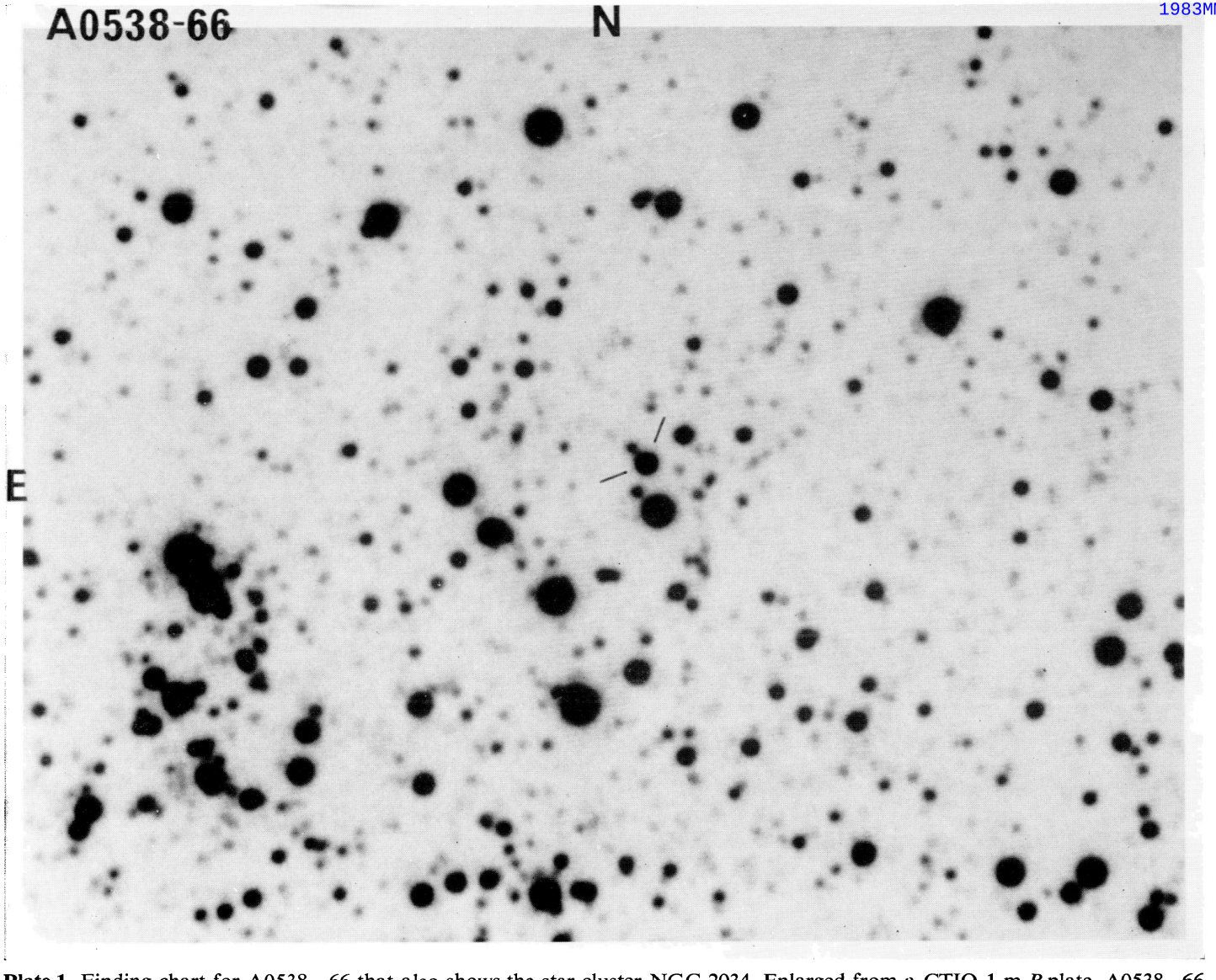

Plate 1. Finding chart for A0538−66 that also shows the star cluster NGC 2034. Enlarged from a CTIO 1-m *B* plate. A0538−66 is star No. 15 in Lucke's Association 772 (a subset of 77, which is Shapley's Constellation III, one of the most active and extended star formation regions in the LMC).

facing page 658

1983MNRAS.202..657C

Downloaded from https://academic.oup.com/mnras/article-abstract/202/3/657/967084
by Dartmouth College Library user
on 26 April 2018

© Royal Astronomical Society • Provided by the NASA Astrophysics Data System

1983MNRAS.202..657C

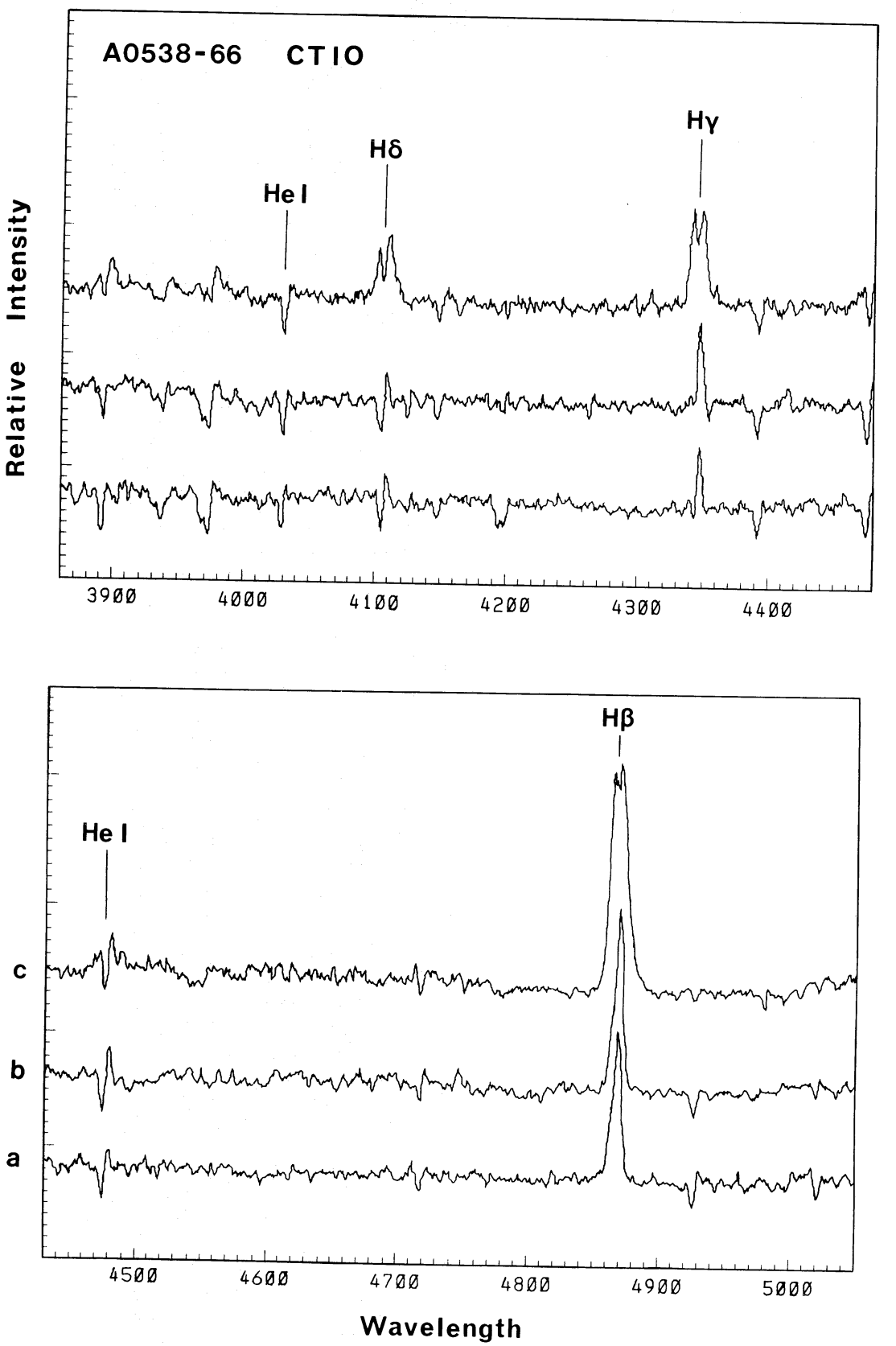

Figure 1. Rectified intensity tracings of spectroscopic plates of A0538 – 66 obtained with the CTIO 4-m and R/C spectrograph on (a) 1980 December 30, (b) 1980 December 31 and (c) 1981 January 1.

Downloaded from http://academic.oup.com/mnras/article-abstract/202/3/657/967884
by Dartmouth College Library user
on 26 April 2018

© Royal Astronomical Society • Provided by the NASA Astrophysics Data System

1983MNRAS.202..657C

Table 1. Journal of observations of A0538 – 66.

Date	UT¶	Phase‡	Telescope/instrument	V (or B)	U–B	B–V	V–R	Spectrum	Observer
1980 Dec 27–29			CTIO 1-m Image Tube	(~15)★★					PAC, LB, RHD, JRT
1980 Dec 30			CTIO 4-m R/C Spectrograph and Image Tube (47 Å mm^{-1})	(~15)††				Fig. 1(a)	PAC, LB, RHD, JRT
1980 Dec 31			CTIO 4-m R/C Spectrograph and Image Tube (47 Å mm^{-1})					Fig. 1(b)	PAC, LB, RHD, JRT
1981 Jan 1			CTIO 4-m R/C Spectrograph and Image Tube (47 Å mm^{-1})	(~14–14.5)††				Fig. 1(c)	PAC, LB, RHD, JRT
1981 Jan 2	0213	(71) 0.02	CTIO 36-in. and comp. photometer	13.27	–	0.06	–		EO
	0334	0.03	CTIO 36-in. and comp. photometer	13.35	–	0.06	–		EO
	0602	0.04	CTIO 4-m R/C and SIT (low resolution)	–	–			see text	J. Baldwin†
	0718	0.04	CTIO 36-in. and comp. photometer	13.00	–	0.03	–		EO
1981 Jan 3	0222	(71) 0.08	CTIO 36-in. and comp. photometer	14.27	–	0.02	–		EO
	0727	0.10	CTIO 36-in. and comp. photometer	14.34		0.09	–		EO
	1242	0.11	AAT/IPCS (66 Å mm^{-1})	–				Fig. 3	R. Terlevich★
1981 Jan 4	0300	(71) 0.14	CTIO 36-in. and comp. photometer	14.71	–0.93	–0.03	0.16		PAC, LB, RHD, JRT
	0447	0.15	CTIO 36-in. and comp. photometer	14.74	–0.86	–0.05	0.15		PAC, LB, RHD, JRT
	0720	0.16	CTIO 36-in. and comp. photometer	14.78	–0.87	0.00	0.13		PAC, LB, RHD, JRT
1981 Jan 5	0245	(71) 0.20	CTIO 36-in. and comp. photometer	14.77	–0.86	–0.07	0.09		PAC, LB, RHD, JRT
	0402	0.21	CTIO 36-in. and comp. photometer	14.84	–0.77	–0.14	0.24		PAC, LB, RHD, JRT
1981 Jan 6	0150	(71) 0.26	CTIO 36-in. and comp. photometer	14.96	–0.87	–0.05	0.11		PAC, LB, RHD, JRT
	0540	0.27	CTIO 36-in. and comp. photometer	14.92	–0.80	0.00	0.13		PAC, LB, RHD, JRT
	0640	0.27	CTIO 36-in. and comp. photometer	14.95	–0.81	–0.02	0.10		PAC, LB, RHD, JRT
1981 Jan 10		(71)	AAT/IPCS (25 Å mm^{-1})	(~15)††					M. M. Phillips†
1981 Jan 11	1630	(71) 0.60	AAT/IPCS (33 Å mm^{-1})	(~15)††				Fig. 4	PAC, LB, RHD

Downloaded from https://academic.oup.com/mnras/article-abstract/202/3/657/987884 by Dartmouth College Library user on 26 April 2018

© Royal Astronomical Society • Provided by the NASA Astrophysics Data System

Downloaded from https://academic.oup.com/mnras/article-abstract/202/3/657/1038888
by Dartmouth College Library
on 26 April 2018

© Royal Astronomical Society • Provided by the NASA Astrophysics Data System

1983MNRAS.202..657C

1981 Jan 12	1225	(71) 0.65	AAT/IPCS (33 Å mm^{-1})	(~15)††					PAC, LB, RHD
1981 Jan 13	0927	(71) 0.70	*IUE* SWP 11042 (180 min)	(≳15)				Fig. 6	AJW
	1252	0.71	*IUE* LWR 9704 (100 min)	(≳15)				Fig. 6	AJW
1981 Apr 29	0327	(78) 0.05	*IUE* SWP 13834 (45 min)	(12.75)§				Fig. 7	AJW
	0408	0.05	*IUE* LWR 10467 (30 min)	(12.70)					
	0447	0.06	*IUE* SWP 13835 (40 min)	(12.74)				Fig. 7	AJW
	0526	0.06	*IUE* LWR 10468 (30 min)	(12.77)					
	0608	0.06	*IUE* SWP 13836 (40 min)	(12.76)				Fig. 7	AJW
	0643	0.06	*IUE* LWR 10469 (20 min)	(12.71)					
	0720	0.06	*IUE* SWP 13837 (40 min)	(12.73)				Fig. 7	AJW
	0801	(78) 0.06	*IUE* LWR 10470 (20 min)	(12.73)					
	0832	0.06	*IUE* SWP 13838 (20 min)	(12.81)				Fig. 7	AJW
1981 July 22	1950	(83) 0.14	MSSSO 1-m and comp. phot.	13.02	−0.49	0.19	–		PAC, LB
1981 July 24	1900	0.26	AAT/IPCS (57 Å mm^{-1})	(≲13)††				Fig. 5	PAC, LB

Errors (for magnitudes *not* given in parentheses) are ~0.02 in V and ~0.05 in the colours, except for the July observation where we estimate the errors to be ~0.05 and 0.1 respectively because of the (necessarily) large air mass through which the star was observed.

Notes

★ At the request of GKS.
† At the request of PAC.
‡ Values of N (in parentheses) are flare cycles and phase computed using ephemerides of phase 0 (flare max) = JD 2 443 423.96 + 16.6515 N (Skinner 1981).
§ Estimated V magnitude from the *IUE* fine error sensor (FES) count rate using relation given by Stickland (1980).
¶ Mid-point of observation.
★★ From photographic plates.
†† Visual estimates from TV guider by comparison with stars in field.

1983MNRAS.202..657C

Our first spectra were obtained from December 30–January 1 with the CTIO 4-m R/C spectrograph and image tube camera on baked IIIa-J plates at a dispersion of 47 Å mm^{-1}. These plates were scanned with the Berkeley PDS microdensitometer to yield the spectra displayed in Fig. 1. On the first night (December 30) the TV guiding system showed the star to be at, or near, its quiescent magnitude, but the Balmer and He I emission indicated the presence of growing activity. The early-type absorption spectrum seen by Johnston *et al.* is also evident. By the third night (January 1) it was clear from the TV that the star had brightened (by ~ 0.5–1 mag). The emission features now dominate the spectrum, exhibiting P Cygni profiles and considerable width (~ 1000 km s^{-1}). The absence of any He II λ4686 is notable, this line being almost always present in the powerful galactic X-ray sources of both high and low mass (see e.g. McClintock, Canizares & Tarter 1975).

On January 2 we commenced a series of *UBVR* photometric observations over five nights with the CTIO 36-in. telescope and computer photometer. The results are plotted in Fig. 2. We were also fortunate in acquiring (courtesy of Dr J. Baldwin) a short exposure, low resolution (~ 25 Å), SIT Vidicon spectrum. This observation was made with the 4-m telescope and R/C spectrograph approximately 1½ hr after the January 2 photometric measurement of the optical maximum in the light curve. Only broad emission lines are evident, principally the Balmer series, but the *strongest* feature is now He II λ4686 with an equivalent width of ~ 36 Å. Given the low resolution this spectrum is consistent with that shown in Fig. 3 (see Section 2.2).

Observing conditions throughout this entire period at CTIO were perfectly photometric with good seeing (~ 1 arcsec), and the colours are accurate to ~ 0.05 mag and V to ~ 0.02 mag.

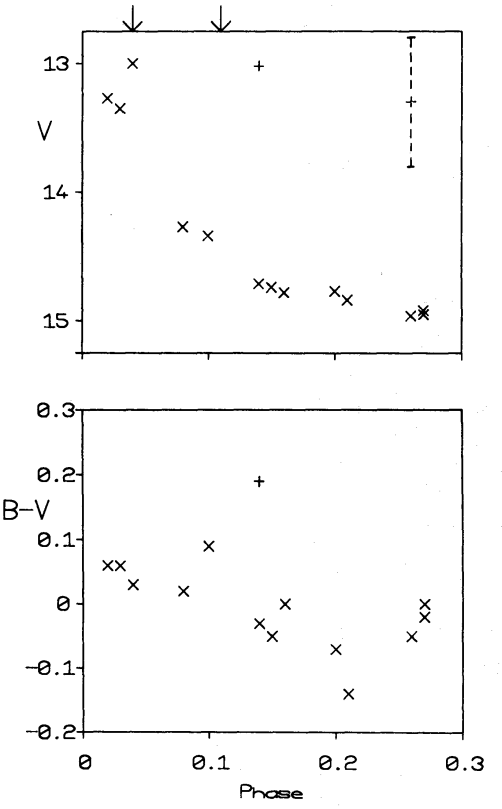

Figure 2. Magnitudes and colours of A0538 – 66 obtained with the CTIO 36-in. and computer photometer. Arrows refer to the times of the spectra shown in Fig. 3 and discussed in the text.

Downloaded from https://academic.oup.com/mnras/article-abstract/202/3/657/967984
by Dartmouth College Library user
on 26 April 2018

© Royal Astronomical Society • Provided by the NASA Astrophysics Data System

1983MNRAS.202..657C

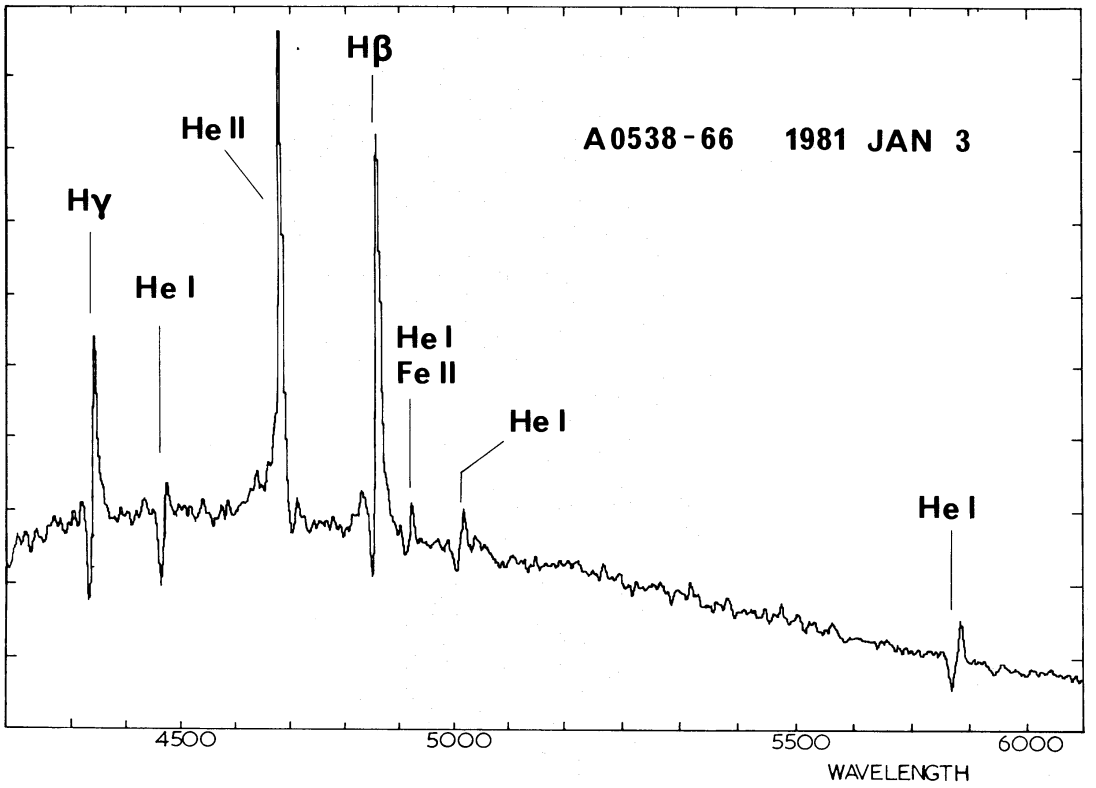

Figure 3. AAT/IPCS spectrum (at ~ 3.5 Å resolution) of A0538 – 66 obtained by R. Terlevich two days after the outburst peak. Note the complex P-Cygni profiles with underlying broad components and the powerful, but narrow, He II λ 4686 compared with Fig. 1(c).

We obtained approximately 1 hr of data in the *U* band (on January 3 and 4) with 2-s integrations to search for any periodicities and short time-scale variability by means of an FFT analysis. No regular fluctuations were found with an upper limit of ~ 5 per cent in the range 4 s–15 min. This limit was set by adding a sinusoidal signal of variable amplitude to the data-set until it was visible in the power spectrum. The spectrum was consistent with white noise.

2.2 AAO (1981 January 3, 10–12)

Further spectroscopic observatons of A0538 – 66 during the January outburst cycle were obtained with the 3.9-m Anglo-Australian telescope (AAT) and IPCS with the RGO spectrograph (see Table 1).

The January 3 spectrum is displayed in Fig. 3 (its time and that of the CTIO January 2 spectrum are marked on Fig. 2). It is dominated by Balmer and He I lines with more accentuated P Cygni profiles than those of Fig. 1. He II λ 4686 emission is still very strong, and the C III/N III band at λλ 4640 – 50 is discernible as a weak, broad feature. At Hβ and Hγ (and perhaps some of the He lines) there is an underlying broad emission component (FWHM ~ 3000 km s^{-1}). The velocities have been estimated by simultaneously fitting Gaussian profiles to the emission and absorption components (and where appropriate the broad component and adjacent lines) to produce the results of Table 2. The velocity accuracy is ± 40 km s^{-1} with an additional systematic uncertainty of ~ 50 km s^{-1}. This means

Downloaded from https://academic.oup.com/mnras/article-abstract/202/3/657/967984
by Dartmouth College Library user
on 26 April 2018
© Royal Astronomical Society • Provided by the NASA Astrophysics Data System

1983MNRAS.202..657C

Table 2. A0538 – 66 velocity components (January 3).

Feature		Velocity★ km s^{-1}	FWHM† km s^{-1}
Emission	H	560	340
	He I	560	300
	He II	450	240
Absorption	H	−315	640
	He I	−300	450

Notes

★ Random errors on the velocity measurements are about ± 40 km s^{-1}, but due to calibration uncertainties an additional systematic error (of $\lesssim$ 50 km s^{-1}), affecting all measurements in the same way, may be present in this case.

† Approximate corrections have been applied for the effects of the instrumental resolution (3.5 Å).

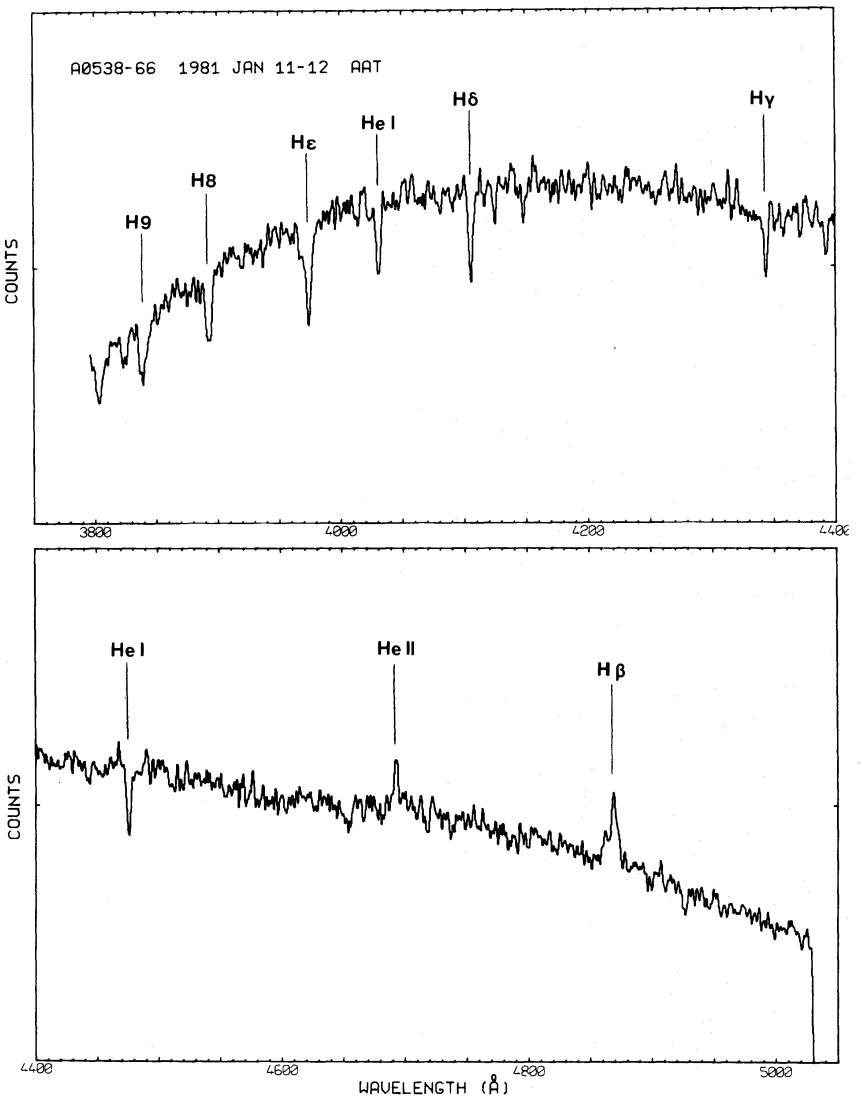

Figure 4. The sum of all our AAT/IPCS spectra of A0538 – 66 obtained on 1981 January 11 and 12 (at ~ 1.5 Å resolution) around phase 0.5 in the 16.6 day outburst cycle. The B2 absorption spectrum is clearly evident together with the peak He II and Hβ emission. Note the weak broad dip at Hγ.

Downloaded from http://academic.oup.com/mnras/article-abstract/202/3/657/967884
by Dartmouth College Library user
on 26 April 2018

© Royal Astronomical Society • Provided by the NASA Astrophysics Data System

1983MNRAS.202..657C

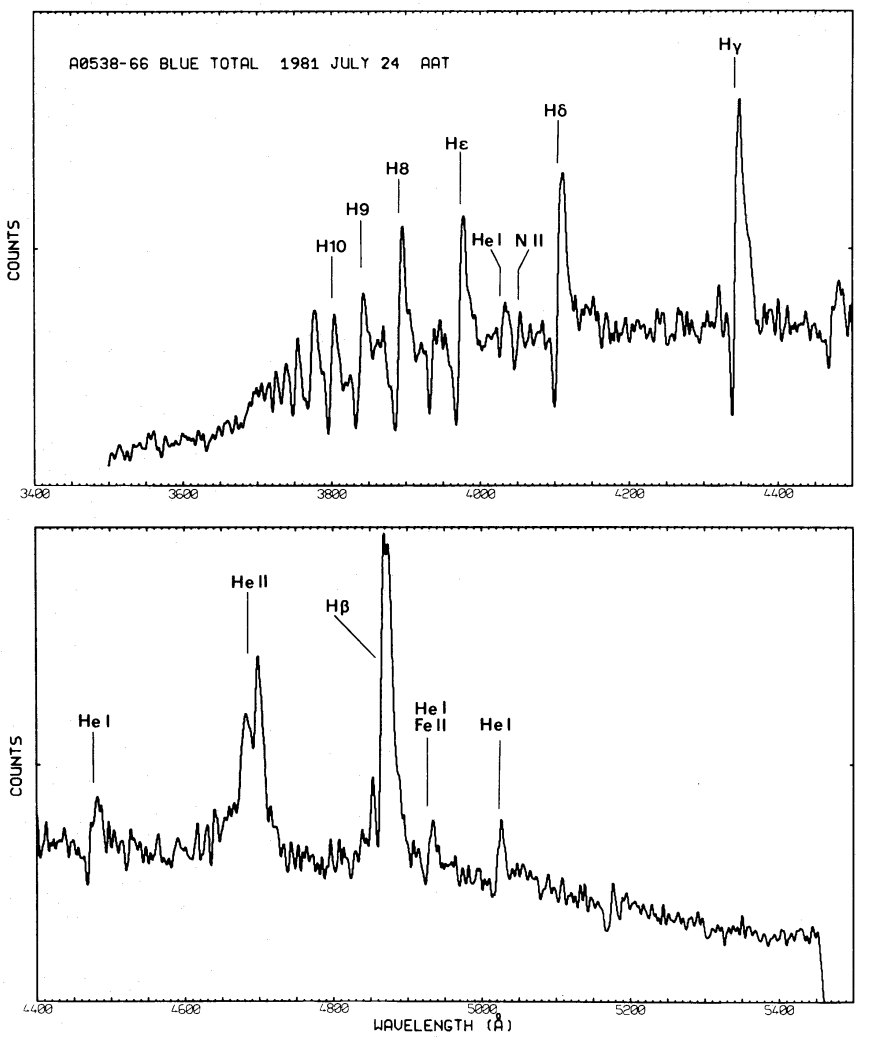

(a)

Figure 5. AAT/IPCS spectra (at ~ 3.5 Å resolution) of A0538 – 66 unusually bright in spite of it being at phase ~ 0.25. Note the double absorption P-Cygni profiles and the complex and broad He II λ 4686 emission (*cf.* Fig. 3).

that the line velocities are of insufficient accuracy to investigate any trend with ionization potential as has been seen in galactic Be stars (see e.g. Hutchings 1976).

The sum of our observations on January 11 and 12 yielded the spectrum shown in Fig. 4. Even though this is now phase 0.5 in the 16.6 day cycle there is clearly some residual activity. Note especially the weak, sharp He II λ 4686 (EW = 0.4 Å) which is almost 500 times weaker in intensity than on January 2.

2.3 MSSSO/AAO (1981 July 22, 24)

During a subsequent observing run at Siding Spring in 1981 July we again observed A0538 – 66 at the time of outburst. We used the Mt Stromlo and Siding Spring Observatories' 1-m telescope and computer photometer system. The tube was a dry ice cooled 1P21 with a matching filter set to reproduce the Johnson *UBV* passbands. Observing conditions were photometric but seeing was ~ 3–4 arcsec, and so we used an 18 arcsec diaphragm. Reference to Plate 1 will show that this implies that we also had some contribution from two faint stars (both with $B > 17$, neither of which is visible on the Johnston *et al.* chart;

Downloaded from http://academic.oup.com/mnras/article-abstract/202/3/657/967784
by Dartmouth College Library user
on 26 April 2018
© Royal Astronomical Society • Provided by the NASA Astrophysics Data System

1983MNRAS.202..657C

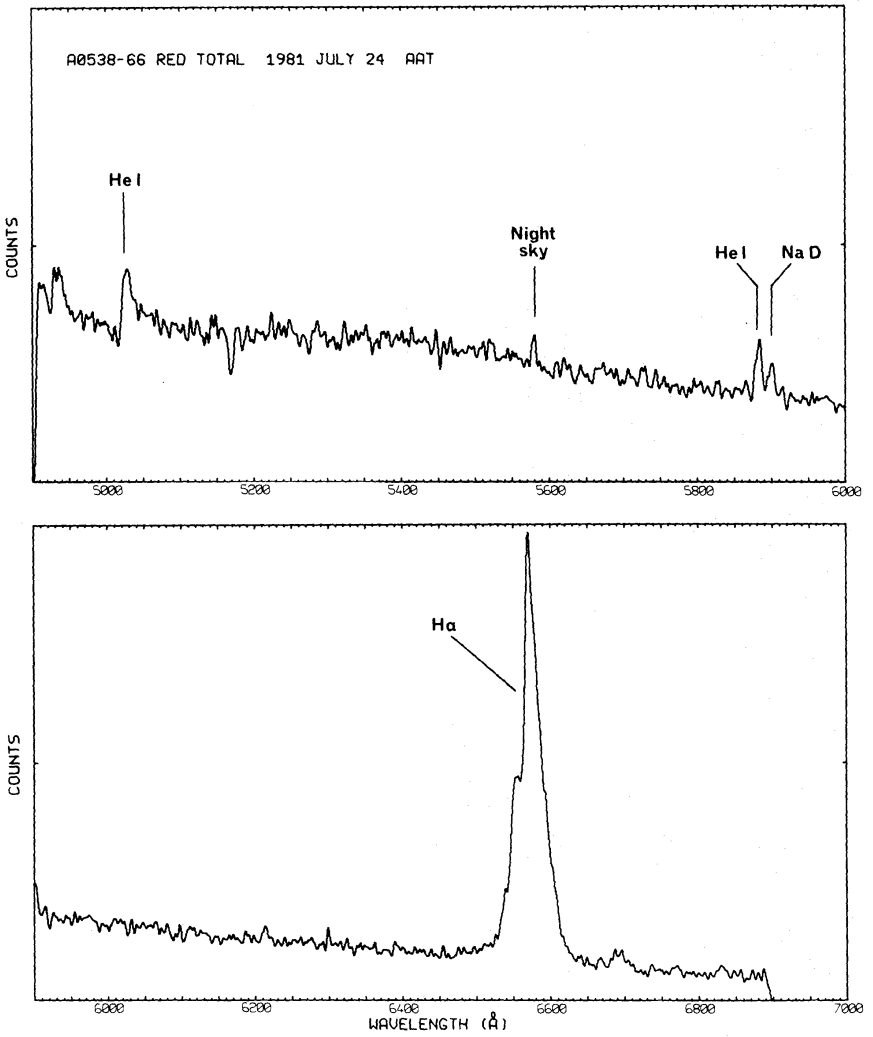

(b)

Figure 5 – *continued*

to the north-east and south-east of A0538 – 66) in the aperture with A0538 – 66. However, since A0538 – 66 was in outburst the contribution of these two stars was negligible. It was relatively straightforward to ensure that stars D and R did not contaminate the observations. Our mean magnitude and colours are included in Table 1. In spite of the large errors associated with these data (due to the large hour angle of the observations) it is clear that (a) the reduced UV excess at maximum is a real effect, and (b) on this occasion the star has undergone an unusually *long* and powerful outburst (compare the magnitudes at the same phase in January).

This latter effect proved to be even more dramatic when we moved to the AAT/IPCS combination on July 24. Visual inspection of the TV guider screen indicated that A0538 – 66 was *at least* as bright as star R (Johnston *et al.*) implying $V \sim 13.3$. Unfortunately, the spectra we obtained (see Fig. 5) could not be reduced to absolute fluxes because observing conditions were far from photometric.

2.4 ULTRAVIOLET SPECTROPHOTOMETRY

IUE observations were obtained at the European observatory (VILSPA) when the source was in quiescence 1981 January 13 and subsequently during outburst on 1981 April 29 as

Downloaded from https://academic.oup.com/mnras/article-abstract/202/3/657/967884
by Dartmouth College Library user
on 26 April 2018
© Royal Astronomical Society • Provided by the NASA Astrophysics Data System

1983MNRAS.202..657C

detailed in Table 1. At both epochs low-resolution UV spectrophotometry ($\Delta\lambda \sim 6$ Å) was obtained in both the short wavelength (SWP camera λλ 1150–2000) and long wavelength (LWR camera: λλ 1850–3250) spectrographs. All data were secured with the source located in the large (10 x 20 arcsec) apertures to ensure photometric integrity in the data. We have reduced the data (Snijders 1980; Giddings 1981) to the form of absolute flux spectrophotometry using the calibrations provided by Bohlin *et al.* (1980). Below we investigate variations in the UV energy distribution of A0538 – 66 from quiescence to flaring.

2.4.1 *Quiescence* (1981 January 13)

At this epoch A0538 – 66 could not be seen in the field of view of the *IUE* Fine Error Sensor (FES), indicating it to be fainter than $V \gtrsim 14.5$, consistent with contemporaneous optical photometry ($V = 15.0$, Table 1). The combined spectra obtained at quiescence are shown together in their flux calibrated form in Fig. 6. Although the LWR region is comparatively featureless, the SWP spectrum shows pronounced P-Cygni profiles in N V λ 1240, Si IV λ 1400 and C IV λ 1550, as well as absorptions due to Si II λ 1260, O I λ 1302 and C II λ 1335.

The P Cygni profiles have velocities associated with the centres of their displaced absorption components of $1150 \pm 130\,\mathrm{km\,s^{-1}}$, and violet absorption edge velocities of $\sim 2400\,\mathrm{km\,s^{-1}}$. Castor, Lutz & Seaton (1981) have shown from deconvolutions of *IUE* low-resolution spectra, that the true edge velocity is expected to be $\sim 500\,\mathrm{km\,s^{-1}}$ less than this. After correcting for this, plus the effect of instrumental resolution and the LMC redshift, we infer that at quiescence A0538 – 66 has a stellar wind with a terminal velocity of $V_\infty = 1640 \pm 200\,\mathrm{km\,s^{-1}}$.

2.4.2 *Outburst* (1981 April 29)

A sequence of additional low-resolution spectra were obtained on 1981 April 29 at phase ~ 0.05 in the 16.6 day cycle. The source had brightened in the visible considerably and was now observable with the *IUE* FES. Throughout the VILSPA shift of April 29 a sequence of SWP spectra followed by LWR spectra were obtained (see Table 1) and prior to each exposure the FES count of the source was used to provide an estimate of its optical brightness.

A montage of the SWP spectra, encompassing regions of special interest, is shown in Fig. 7. The UV spectrum has dramatically changed from that at quiescence (*cf.* Fig. 6) and is now dominated by numerous, strong, broad emission lines. The principal features are N V λ 1240, Si IV λ 1400–O IV λ 1400, C IV λ 1500, He II λ 1640 and O III λ 1663 and are unlike those observed in *any other* galactic or LMC high-mass X-ray binary source (Hammerschlag-Hensberge 1980). UV observations of low mass X-ray sources (e.g. Gursky *et al.* 1980; Willis *et al.* 1980) do show emission in the above species but the lines are much narrower than observed in A0538 – 66.

The great breadth and high velocities of the emission lines is clear from Fig. 8 which shows the profiles of C IV λ 1550 and He II λ 1640 in SWP 13835. The C IV λ 1550 profile shows an absorption component at λ 1544.4 corresponding to a displaced velocity of $\sim 1000\,\mathrm{km\,s^{-1}}$. This value is similar to that inferred from the P Cygni profile seen at quiescence and we suggest that the absorption in C IV λ 1550 at outburst is this same stellar wind component. Both C IV λ 1550 and He II λ 1640 profiles have red wings extending to $\sim +3000\,\mathrm{km\,s^{-1}}$, that of the latter merging with O III λ 1663. There is evidence from Fig. 8 that C IV and He II profiles are asymmetric with violet wings extending to higher velocities of ~ -5500

Downloaded from http://adsabs.harvard.edu/cgi-bin/nph-article_abstract/202/3/657/4967884
by Dartmouth College Library user
on 26 April 2018

© Royal Astronomical Society • Provided by the NASA Astrophysics Data System

1983MNRAS.202..657C

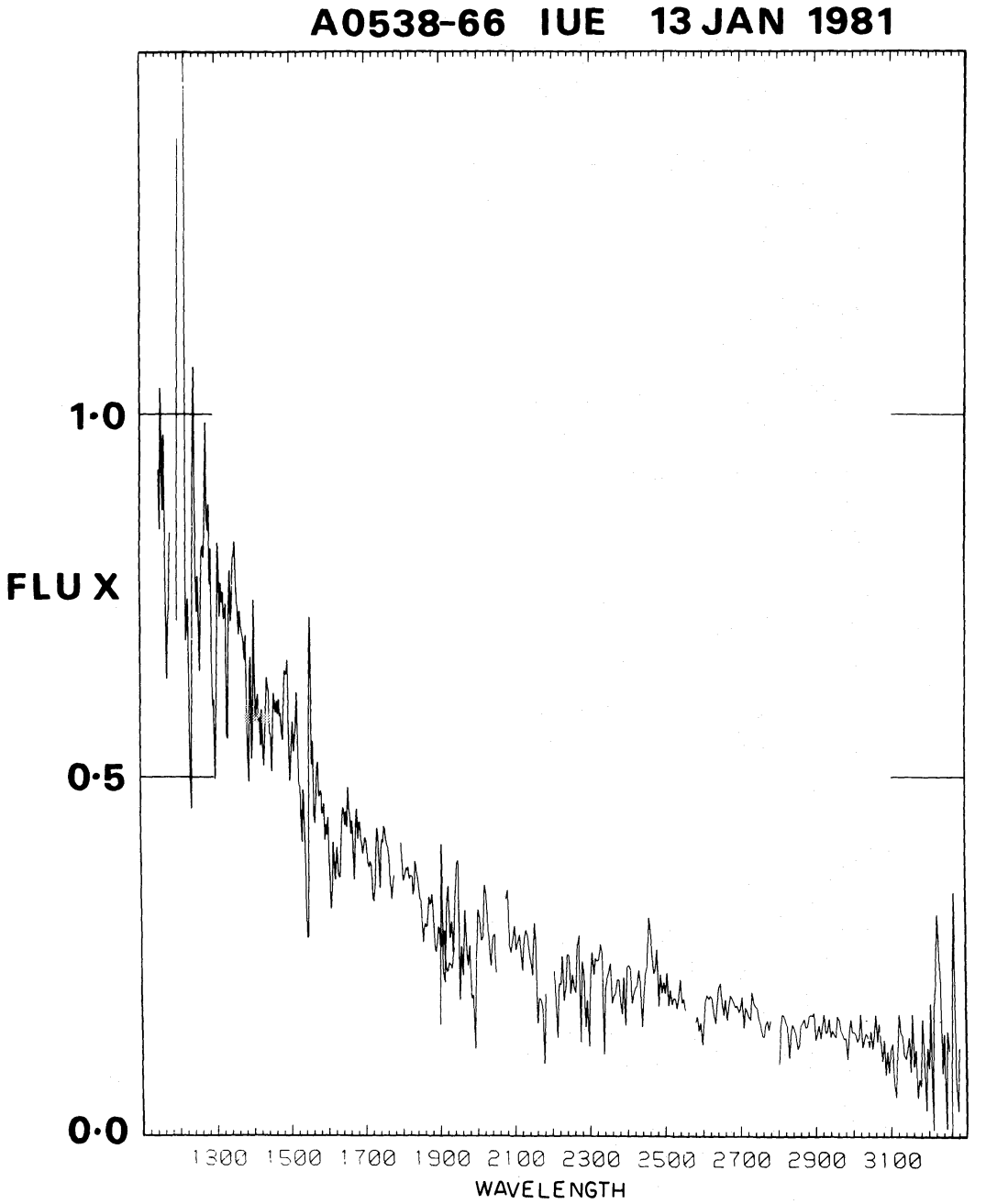

Figure 6. The combined SWP 11042 + LWR 9704 low-resolution *IUE* spectrophotometry of A0538 – 66 obtained on 1981 January 13 with the source in quiescence. The ordinate scale is $10^{13} F_\lambda$ (erg cm^{-2} s^{-1} Å^{-1}).

km s^{-1}: a similar value being indicated by *both* lines. Possible blending effects due to N v λ 1616, λ 1620 may contribute to some of the apparent asymmetry in the case of He II λ 1640, but no likely blending transitions are identified to explain that of C IV λ 1550. The similarity of the inferred extreme violet velocities for the C IV and He II profiles suggest that the asymmetry is real, and as such needs to be explained in any model of the source. It is clear from Fig. 7 that during the course of the data acquisition on April 29 some spectral variations have occurred, accompanying the 30 per cent decrease in the SWP UV continuum (see below). The O III λ 1663 line appears to strengthen relative to He II λ 1640 as the continuum fades (see spectrum E compared to B) and also the width

Downloaded from http://adsabs.harvard.edu/cgi-bin/nph-article_query?bibcode=1983MNRAS.202..657C
by Dartmouth College Library User
on 26 April 2018
© Royal Astronomical Society • Provided by the NASA Astrophysics Data System

1983MNRAS.202..657C

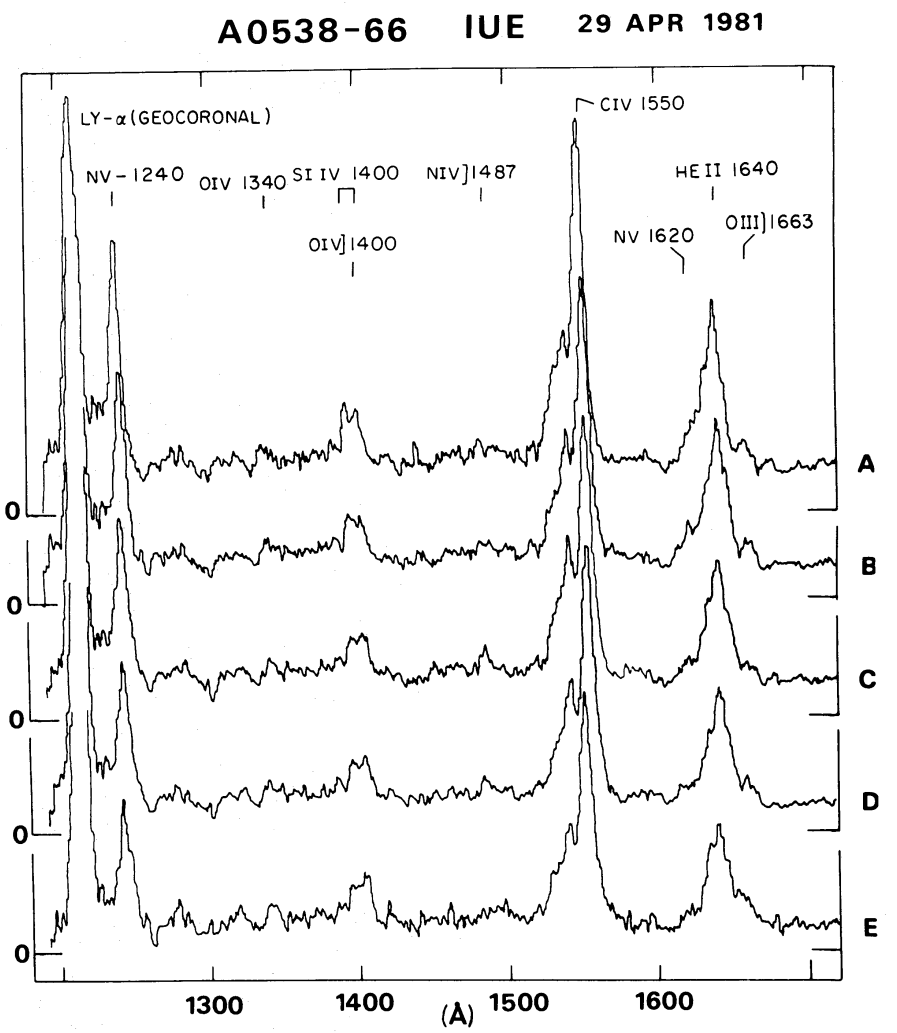

Figure 7. The region λλ 1200–1700 in the five SWP spectra of A0538 – 66 obtained during outburst on 1981 April 29. The spectra are marked in sequence with their acquisition: A = SWP 13834; B = SWP 13835; C = SWP 13836; D = SWP 13837, E = SWP 13838. The ordinate scale in each case is linear intensity with the zero flux levels located in sequence with the spectra. The principal emission lines are identified.

of O III λ 1663 appears to increase and begins to merge with the He II line. This change is accompanied by a reversal in the relative strengths Si IV λ 1400 and O IV λ 1400.

Significant UV brightness changes occurred during the outburst, in addition to the substantial brightening between quiescence and outburst. In order to quantify these UV variations in the continuum, we have isolated the same featureless spectral regions during quiescence. In the SWP range these are: 1270–1290, 1350–1380, 1420–1470, 1490–1520, 1570–1600, 1680–1710, 1770–1840 and 1880–1960 Å. The LWR spectra appear to show no strong features and are assumed to represent the continuum of the source. We have adopted for LWR continuum measurements four 200 Å bands centred at λλ 2025, 2375, 2625 and 2925. For each spectrum the data have been used to determine continuum fluxes, F_λ^c, over each of these wavelength regions. To compare the outburst and quiescent fluxes we form the relations

$$\Delta m_\lambda^c = -2.5 \log \{F_\lambda^c (\mathrm{SWP}x/\mathrm{SWP}\,13834)\}$$

$$\Delta m_\lambda^c = -2.5 \log \{F_\lambda^c (\mathrm{LWR}x/\mathrm{LWR}\,10467)\}.$$

Downloaded from http://adsabs.harvard.edu/cgi-bin/nph-article_query?bibcode=1983MNRAS.202..657C&link_type=ABSTRACT
by Dartmouth College Library User
on 26 April 2018
© Royal Astronomical Society • Provided by the NASA Astrophysics Data System

1983MNRAS.202..657C

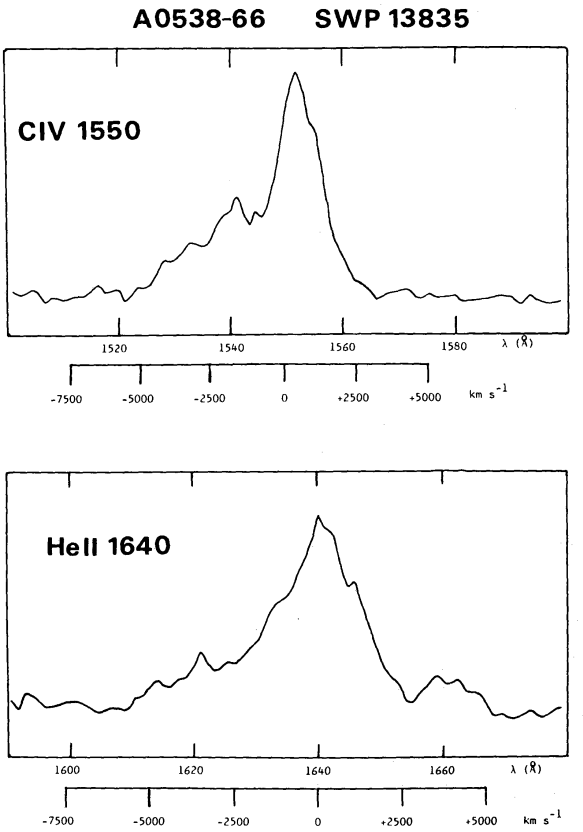

Figure 8. The emission line profiles of C IV λ 1550 and He II λ 1640 + O III λ 1663 observed in the outburst spectrum SWP 13835, plotted on both a wavelength and velocity scale. Both the C IV and He II features appear to be asymmetric with violet wings extending to ~ 5500 km s^{-1}.

The shapes of the individual SWP or LWR spectra are sensibly constant, so in Fig. 9 we plot the mean value of Δm_λ^c for each spectrum against the UT of the start of the exposure. The figure shows that during the course of the April 29 observations A0538 – 66 maintained a near constant UV continuum brightness from 0300–0600, but thereafter decreased in brightness by ~ 30 per cent in the SWP continuum by 0830. There is some evidence from Fig. 9 that the variations in the LWR range lag behind that in the SWP wavelength range, viz the source fades faster at shorter wavelengths. This assertion is strengthened by the apparent near constancy of the FES V magnitude (also plotted in Fig. 9) during outburst. In order to quantify any associated line intensity changes, we have computed

$$F_{\text{line}} = \int_{\text{line}} (F_\lambda - F_\lambda^c)\, d\lambda$$

in erg cm^{-2} s^{-1} for C IV λ 1550 and He II λ 1640 + O III λ 1663. We compare these line intensities with those observed in our first outburst spectrum, converted to the form of a magnitude change in Fig. 9.

No dramatic change in line intensity in the outburst spectra is apparent: in spite of the SWP continuum level drop of 30 per cent at SWP 13838, the lines show a maximum reduction of ~ 10 per cent. This is of the order of the accuracy of the line measurements. Thus the continuum and line emission regions may not be intimately linked.

We have compared the level and shape of the UV continuum between quiescence and outburst using SWP 13835 and LWR 10468 (which show the highest outburst fluxes). The

Downloaded from http://adsabs.harvard.edu/cgi-bin/nph-article_abstract?bibcode=1983MNRAS.202..657C
by Dartmouth College Library user
on 26 April 2018
© Royal Astronomical Society • Provided by the NASA Astrophysics Data System

1983MNRAS.202..657C

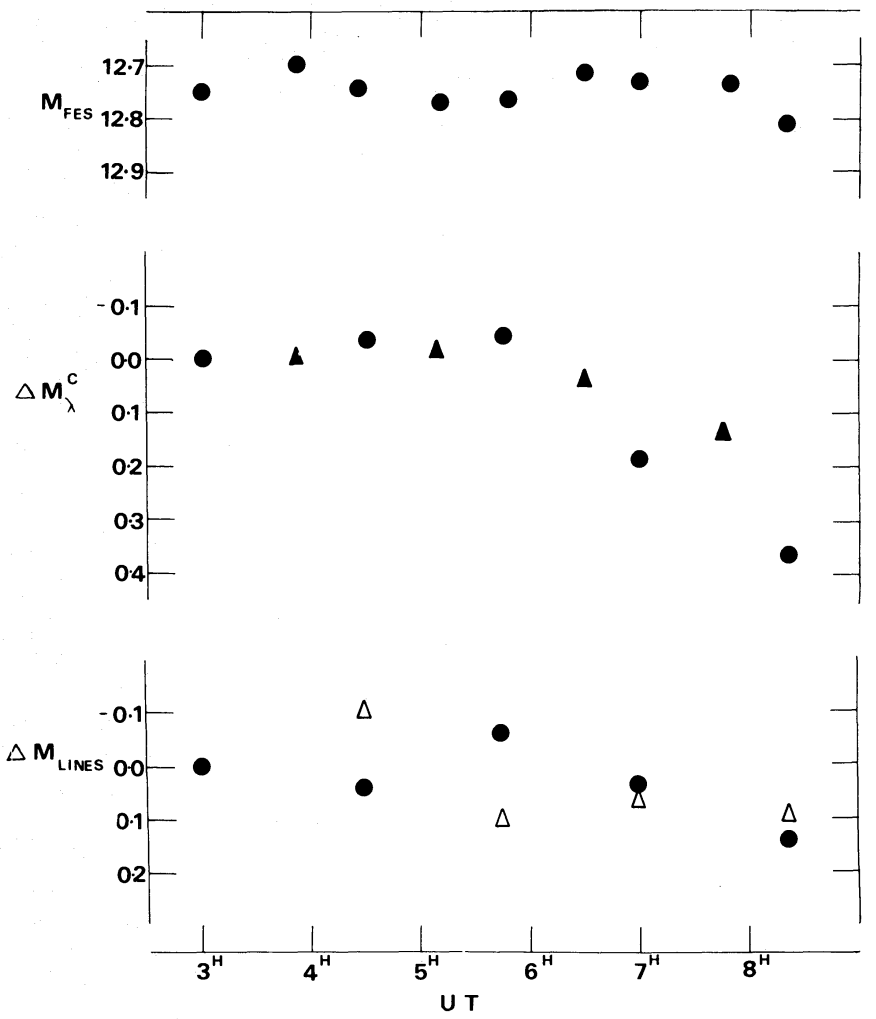

Figure 9. Variations observed with *IUE* for A0538 – 66 during the outburst shift on 1981 April 29 between 0300–0830 UT. Top section: M_{FES} observed before the start of each SWP and LWR observation. Middle section: (•) – the continuum brightness in the SWP observations relative to SWP 13834 and (▲) – the continuum brightness variations in the LWR data relative to LWR 10467. Bottom section: changes in the C IV λ 1550 (•) the He II λ 1640 + O III λ 1663 (△) emission line intensities relative to those observed in SWP 13834.

difference in continuum magnitudes is shown in Fig. 10. It is clear that the source does *not* maintain a constant colour as its brightness changes; the data in Fig. 10 indicate a near monotonic *increase* towards longer wavelengths, from ~ 0.5 mag at 1300 Å to ~ 1.7 mag at 3000 Å. The corresponding change in the visible estimated from our FES V magnitude data and the UBV photometry obtained at quiescence is ~ 2.3 mag.

3 Interpretation

3.1 SPECTRAL TYPE

The reddening in this direction is low and Murdin *et al.* (1981) adopt Dach's (1972) mean values of $E(B-V) = 0.04$ and $E(U-B) = 0.03$. If we take our January 6 observations as representative of the quiescent magnitude (but note the weak remnant emission features) we obtain mean magnitudes and colours of $V = 14.94$, $B-V = -0.02$ and $U-B = -0.83$. With

Downloaded from http://academic.oup.com/mnras/article-abstract/202/3/657/967984
by Dartmouth College Library user
on 26 April 2018

© Royal Astronomical Society • Provided by the NASA Astrophysics Data System

1983MNRAS.202..657C

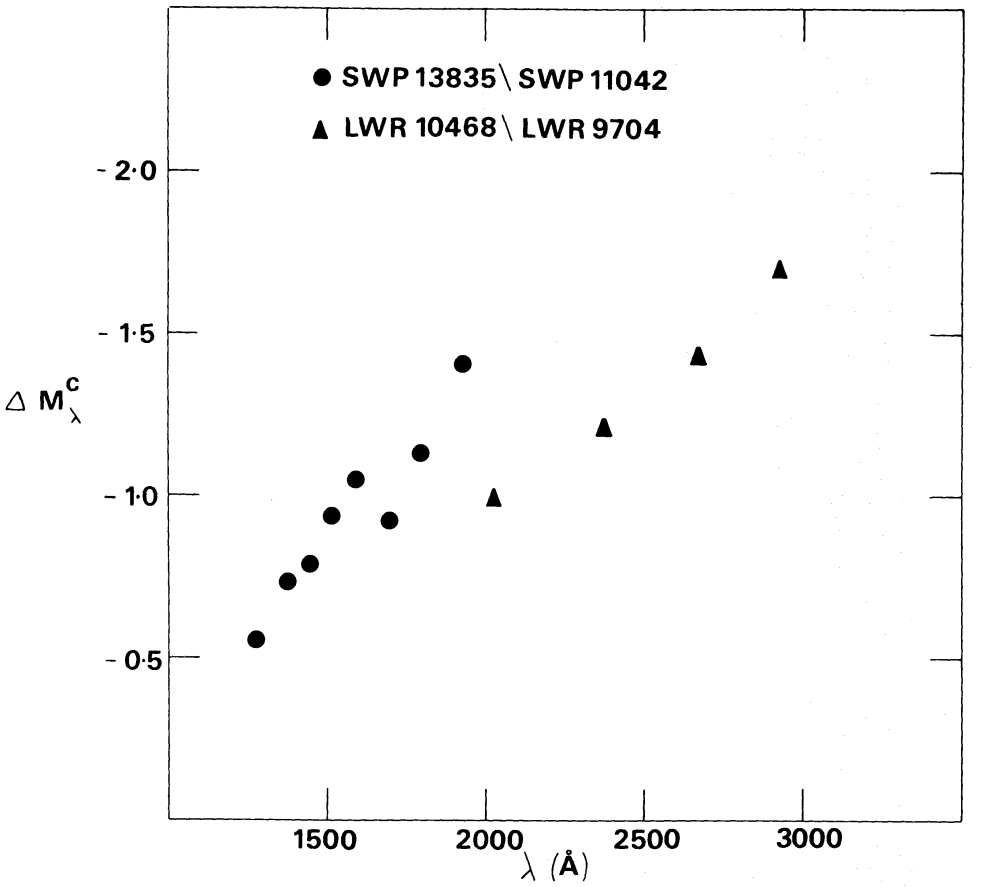

Figure 10. The UV continuum brightness variations observed in the *IUE* wavelength range between quiescence and flare states.

Dach's reddening corrections (which are consistent with the *IUE* spectra) we derive $V_0 = 14.82$, $(B-V)_0 = -0.06$ and $(U-B)_0 = -0.86$. Adopting an LMC distance modulus of 18.6 yields $M_V = -3.78$.

We assign a spectral type of B2 III–IV on the basis of the relative He I, N II, Si II and O II line strengths (Yamashita, Nariai & Norimoto 1977) (but note that these lines were not always consistent with the luminosity classification, as expected for variable emission contributions). The spectral features from all three nights observations were fitted by a least-squares routine to a combined Gaussian–Lorentzian profile to yield the results given in Table 3. All the lines are clearly resolved with widths of 250–450 km s^{-1}.

The *IUE* quiescent spectrophotometry independently indicates that the primary star is not on the main-sequence. Previous UV observations of hot, early-type stars show that substantial mass loss associated with well-developed P Cygni profiles is (at least for B stars) confined to luminous objects of classes III–I (Lamers 1980).

The data of Fig. 6 show little evidence for the interstellar λ2200 band. They are consistent with a low colour excess of $E(B-V) \lesssim 0.05$ arising from interstellar reddening in the Galaxy alone. From an inspection of SWP data we have selected several featureless regions representative of the stellar continuum and have formed UV continuum magnitudes, $U_\lambda = -2.5 \log f_\lambda - 21.10$ (Oke & Schild 1970) which are dereddened with $E(B-V) = 0.05$ using the mean galactic interstellar extinction law from Seaton (1979). We have compared the intrinsic flux distributions of hot early-type stars in the Galaxy (Nandy *et al.* 1976) with the broad-band colours of A0538−66 to estimate the spectral classification. We adopt

Downloaded from http://adsabs.harvard.edu/cgi-bin/nph-article_query?bibcode=1983MNRAS.202..657C
by Dartmouth College Library user
on 26 April 2018
© Royal Astronomical Society • Provided by the NASA Astrophysics Data System

1983MNRAS.202..657C

Table 3. Spectral features of A0538 – 66 from AAT/IPCS.

Line	Δλ Å	FWHM Å	Instrument Å	Corrected FWHM km s^{-1}
He I λ 4026	–	–	–	–
	3.4	5.0	1.6	353
	4.8	4.1	1.4	287
Hδ λ 4100	–	–	–	–
	5.0	5.5	1.4	389
	5.9	4.6	1.5	318
Hγ λ 4340	3.6	4.0	1.9	243
(em. compt.)	4.7	3.6	1.7	219
	4.0	3.7	1.3	239
He I λ 4471	3.6	5.3	1.9	332
(em. compt.)	4.3	5.0	1.6	318
	4.9	4.7	1.6	296
He II λ 4686	6.7	7.2	1.8	446
	7.1	4.6	1.6	276
	7.3	4.1	1.4	247
Hβ λ 4861	8.7	6.4	1.9	377
	8.2	7.6	2.3	447
	8.4	7.0	1.9	416

Notes

The line FWHM is corrected by the instrumental resolution at that wavelength (determined with the same routine applied to arc spectra) to give corrected FWHM in km s^{-1}. The three entries for each line correspond to mean spectra for 1981 January 10, 11 and 12 (see Table 1 and Fig. 6).

$V = 15.0$ for the quiescent magnitude, which with $E(B-V) = 0.05$ gives $V_0 = 14.84$. With the value of $M_v = -3.78$ derived earlier, this indicates a quiescent classification of B2 III, implying $M_{bol} = -5.5$.

Our optical photometry measurements are consistent with the spectral classification of B2 III but it must be noted that we have no accurate *UBV* photometry during an extended 'inactive' period and so colour variations due to differing emission contributions could be present.

The slight 'reddening' at the peak (January 2 compared with January 5) appears to be real. Our *U–B* colour is also noticeably more ultraviolet than that of Murdin *et al.* (1981). It was this lower *U–B* value that resulted in Murdin *et al.* assigning the rather later spectral type of B7 II. In addition they used an Hγ measurement from a spectrum taken at the end of 1981 January to determine M_v. This is likely to be more uncertain than usual because of the residual activity (in Hβ and He II, see Section 2.2) seen outside of maximum at this time.

3.2 CONTINUUM DISTRIBUTION

The results from Fig. 10 indicate that the origin of the enhanced UV and visible continuum emission at outburst is *not* due to: (i) emission in a simple steady accretion disc, for which we would expect $F_\lambda \propto \lambda^{-2.3}$ (see e.g. Bath, Pringle & Whelan 1980) and emission increasing to shorter wavelengths, nor to (ii) emission arising in the X-ray heated atmosphere of the early-type primary star since the outburst spectra show a *decreased* colour temperature compared to that observed at quiescence.

Downloaded from http://adsabs.harvard.edu/cgi-bin/nph-article_query?bibcode=1983MNRAS.202..657C
by Dartmouth College Library user
on 26 April 2018
© Royal Astronomical Society • Provided by the NASA Astrophysics Data System

1983MNRAS.202..657C

The *IUE* continuum regions are well fitted by normal Kurucz model stellar atmospheres assuming $V_0 = 14.84$. The fits are shown in Fig. 11 and give

	Outburst	Quiescence
$T_{\rm eff}$	12 500 K	18 000 K
Sp.	B8–9 I	B2 III
R	$45\,R_\odot$	$11.5\,R_\odot$

which also nicely confirm the quiescent spectral type. From these data and Panagia (1973) we adopt primary B2 III physical parameters of

$M_1 = 12\,M_\odot$

$R_1 = 8 \times 10^{11}$ cm $= 11.5\,R_\odot$

$L_1 = 4.7 \times 10^{37}$ erg s^{-1} $= 1.2 \times 10^4\,L_\odot$.

3.3 RADIAL VELOCITIES

In Fig. 12 we show, plotted against the 16.6 day outburst phase, radial velocities of the more pronounced spectral features from the data presented in Section 2, together with data of Hutchings, Cowley & Crampton (1981 and private communication) and Pakull & Parmar (1981). From this figure we note:

(a) The quiescent spectral absorption features are all consistent with a velocity of $+300$ km s^{-1}, as expected for a member of the LMC.

(b) There are significant changes in the velocity of the He II λ4686, even between different cycles at the same phase.

3.4 THE BINARY PERIOD

Throughout this work we have referred to the recurrent 16.6 day outburst events as a cycle because there is no direct evidence that this cycle actually represents the binary period. We had hoped to search for binary motion in the radial velocity of He II λ4686 under the assumption that it is being produced in the vicinity of the X-ray source. This is supported by our discovery that λ4686 turns on suddenly, well after the optical outburst has started, suggesting that it is being produced in a different region or at least is associated with the X-rays which also turn on after the optical (as also seen in 4U0115+63 by Kriss *et al.* 1982). If we assume that the system consists of a $\sim 12\,M_\odot$ 'B' star and a $1\,M_\odot$ compact object, near which the X-rays are being produced, we would then expect the X-ray object to have a velocity of $\sim 200\,(P/16.6)^{-1/3}$ km s^{-1}. Such a velocity variation is seen but not with any 16.6 day modulation. However, note that the X-ray luminosity is so high that significant X-ray heating of the primary star *and* surrounding material must contribute to the optical emission. This might even be true at times away from the peak luminosity when large column densities have been seen (Skinner 1981) and hence the intrinsic X-ray flux may be much higher. Thus, the precise location of the He II may vary dramatically with the X-ray intensity (see e.g. the huge width and structure of λ4686 in Fig. 5).

In the absence of any other information, we shall assume in our calculations that 16.6 day is indeed the binary period; it does represent a fairly stable clock (Skinner 1981).

Downloaded from http://adsabs.harvard.edu/cgi-bin/nph-article_abstract?bibcode=1983MNRAS.202..657C by Dartmouth College Library user on 26 April 2018

© Royal Astronomical Society • Provided by the NASA Astrophysics Data System

1983MNRAS.202..657C

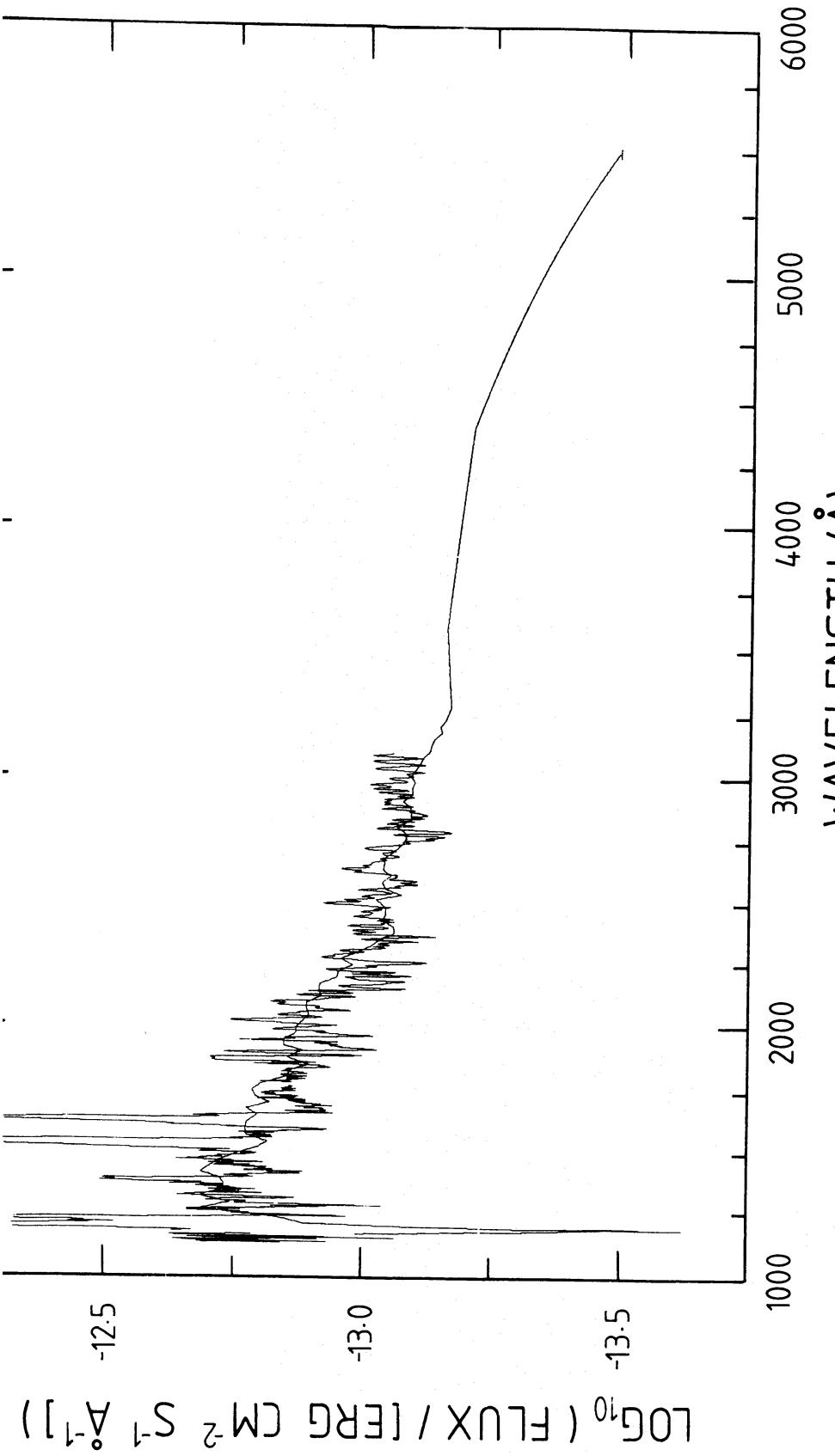

(a)

Figure 11. Model atmosphere fits of the *IUE* data taken during outburst and quiescence. Continuum regions were selected as described in the text. (a) A0538 – 66 at maximum. These data have been smoothed with a 10 Å triangular filter after dereddening an $E(B-V) = 0.04$ using Seaton's law modified for $R = 3.1$. Optical magnitude and colours assumed were $V = 12.73$ (from the FES count), $B-V = 0.05$, $U-B = -0.50$. The best-fit model has $T = 12\,500$ K, $\log g = 2$, $R = 45\,R_\odot$ (at 55 kpc). This 'reddening' (relative to b) implies a much larger emitting region compared to the quiescent B2 III primary. (b) A0538 – 66 at minimum. Similarly smoothed, the V point corresponds to 15.0. The model fit has $T = 18\,000$ K, $\log g = 3.5$, $R = 11.5\,R_\odot$.

Downloaded from https://academic.oup.com/mnras/article-abstract/202/3/657/967984
by Dartmouth College Library user
on 26 April 2018

© Royal Astronomical Society • Provided by the NASA Astrophysics Data System

1983MNRAS.202..657C

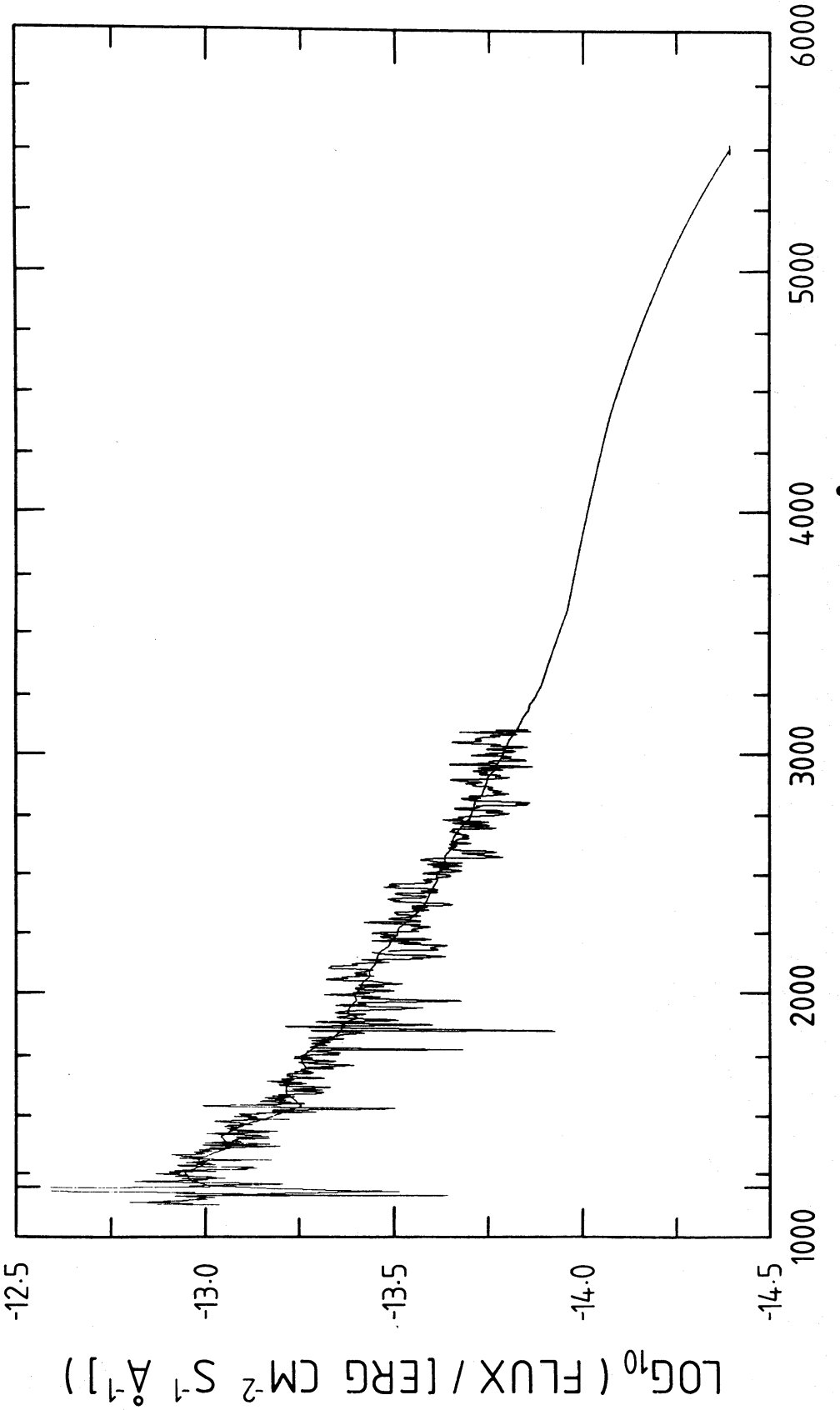

(b)

Figure 11 – *continued*

Downloaded from https://academic.oup.com/mnras/article-abstract/202/3/657/967984
by Dartmouth College Library user
on 26 April 2018

© Royal Astronomical Society • Provided by the NASA Astrophysics Data System

1983MNRAS.202..657C

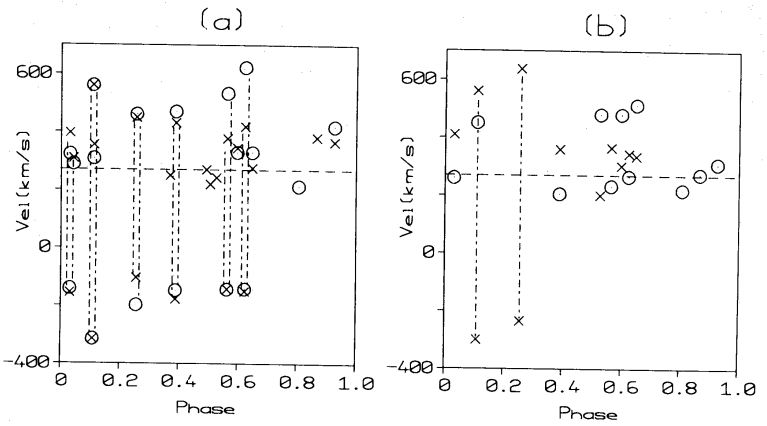

Figure 12. A collection of available velocity measurements of the dominant spectral features in A0538 – 66. They are plotted against phase in the 16.6 day outburst cycle. (a) Hydrogen lines x = Hγ ⊙ = Hδ; (b) Helium lines x = He I ⊙ = He II. The LMC velocity is marked by a dashed line. Emission and absorption peaks of a P-Cygni profile are connected by dotted lines; where there are two absorption components the redder component is shown. Errors are ± 60 km s^{-1} for He II and ± 35 km s^{-1} for the rest.

4 Discussion

Large mass loss is indicated both by the growth of P Cygni profiles in the optical development (Fig. 1) and by their presence in spectra obtained after optical maximum (Figs 3 and 5). Note the very broad (~ 30 Å ≡ 2000 km s^{-1}) He II λ 4686 with a double emission peak in Fig. 5 (*cf.* Fig. 7). Indeed these show a remarkable similarity to P Cygni itself where Abbott, Bieging & Churchwell (1981) infer an $\dot{M}$ of ~ $1.7 \times 10^{-5} M_\odot$ yr^{-1}, with multiple absorption components (as in our Fig. 5) being interpreted as due to absorption in different shells of the expanding atmosphere.

It must be borne in mind that, since $L_{\rm Edd} \sim 10^{38} (M_{\rm x}/M_\odot)$ erg s^{-1}, A0538 – 66 is radiating (at peak) ~ $10\, L_{\rm Edd}$ if the compact object is indeed a $1 M_\odot$ neutron star. However, the presence of a powerful magnetic field is indicated by an increase in the optical polarization observed at outburst (Clayton & Thompson 1981). A supercritical accretion flow will greatly complicate the interpretation outlined below.

4.1 MASS TRANSFER PROCESS

If a compact object of radius R and mass $M_{\rm x}$ accretes material at a rate $\dot{M}$ then the resulting X-ray luminosity will be $L_{\rm x} = GM_{\rm x}\dot{M}/R$ and assuming that the compact object is a $1 M_\odot$ neutron star, then $L_{\rm x} = 6 \times 10^{45} \dot{M}$ erg s^{-1} where the mass transfer rate, $\dot{M}$, is in $M_\odot$ yr^{-1}. Thus, for a peak $L_{\rm x} \sim 10^{39}$ erg s^{-1}, we require at least $\dot{M} \sim 1.7 \times 10^{-7} M_\odot$ yr^{-1}, ignoring the limiting effects of radiation pressure. This has to be the amount of material actually *accreted* by the compact object. What is the mechanism by which this material is transferred? The transient nature of the source requires that the process is discrete with a time variation at least as short as the time-scale for the basic X-ray variability. Such a large variation as is observed strongly suggests an *eccentric* rather than a circular orbit.

As a source of material in this eccentric binary we will consider two extreme possibilities; stellar wind and overflow of the primary's tidal lobe.

4.1.1 Wind accretion

The Bondi–Hoyle accretion model was first applied to galactic X-ray sources by Davidson & Ostriker (1973). The fraction f of material accreting on to the neutron star from the

Downloaded from https://academic.oup.com/mnras/article-abstract/202/3/657/967984
by Dartmouth College Library user
on 26 April 2018
© Royal Astronomical Society • Provided by the NASA Astrophysics Data System

1983MNRAS.202..657C

primary and the resulting X-ray luminosity for the general case of an eccentric orbit are given in Avni & Goldman (1980). The variation of the wind velocity v_w with r is still subject to considerable debate (e.g. Barlow 1982). We investigate two extreme velocity laws: the steep velocity profile of Castor, Abbott & Klein (1975)

$$\frac{v_w}{v_\infty} = \left(1 - \frac{R_1}{r}\right)^{1/2} \qquad \text{(C)}$$

and the much more gradual one of Barlow & Cohen (1977)

$$\frac{v_w}{v_\infty} = \left(1 - \frac{R_1}{r}\right)^{0.21} 10^{-1.74(R_1/r)} \qquad \text{(BC)}$$

where v_∞ is the terminal velocity of the stellar wind (at $r = \infty$). Applying these two velocity laws to A0538 – 66 leads to the results summarized in Table 4 for $\dot{M}_1 = 10^{-5} M_\odot\ \mathrm{yr}^{-1}$ and $e = 0.77$ (see next section). We have used our measured value of $v_\infty = 1640\ \mathrm{km\ s}^{-1}$ (Section 2.4.1).

Clearly, if the primary's mass loss rate can be as high as $\dot{M}_1 \sim 10^{-5} M_\odot\ \mathrm{yr}^{-1}$ the BC law is capable of giving a high enough wind density at periastron to (potentially) produce large X-ray luminosities, L_x (max).

Previous observations of L_x (min) during outbursts were undertaken by pre-*Einstein* satellites and so give upper limits of only $\sim 10^{36-37}\ \mathrm{erg\ s}^{-1}$, giving a max–min ratio which can be accommodated by either velocity law. However, two *Einstein* observations of this region were conducted in 1980 during the 'inactive' period of A0538 – 66 and also yielded only upper limits (see Skinner 1981). In the 0.5–4 keV band these limits are $\sim 10^{35}\ \mathrm{erg\ s}^{-1}$ (Long, Helfand & Grabelsky 1981) and are useful because the max–min ratio cannot be accommodated by either velocity law. This conclusion depends only on the assumption that (a) during times of X-ray inactivity, the primary star behaves like a 'normal' early-type star and will have a residual stellar wind similar to stars with the same physical parameters (Lamers 1981 relates the mass loss rate to the stellar M, L and R which, for A0538 – 66, yields $\dot{M} = 3.8 \times 10^{-8} M_\odot\ \mathrm{yr}^{-1}$); and (b) the X-ray source is not heavily obscured (the possibility of which can be ruled out on optical grounds). Thus, although the stellar wind accretion model *can* satisfy some of the constraints of this system we believe it is unlikely to provide a viable model. In particular it would have considerable difficulty accounting for the shape of the X-ray light curve.

Murdin *et al.* (1981) consider a variation on this model in the form of X-ray modulation by varying photoelectric absorption in the primary's wind caused by the eccentric orbit

Table 4. Wind accretion calculations for A0538 – 66.

	Periastron		Apastron	
Velocity law	C	BC	C	BC
r	1.04×10^7	1.04×10^7	7.97×10^7	7.97×10^7 km
v_x	540	540	71	71 km s^{-1}
v_w	790	55	1560	1070 km s^{-1}
f	1.1×10^{-4}	0.009	2.2×10^{-7}	10^{-6}
L_x	9.6×10^{37}	7.4×10^{38}	1.9×10^{34}	8.4×10^{34} erg s^{-1}
$\frac{L_x\ (\mathrm{max})}{L_x\ (\mathrm{min})}$ C		500		
$\frac{L_x\ (\mathrm{max})}{L_x\ (\mathrm{min})}$ BC		9000		

Downloaded from http://academic.oup.com/mnras/article-abstract/202/3/657/967884
by Dartmouth College Library user
on 26 April 2018

© Royal Astronomical Society • Provided by the NASA Astrophysics Data System

1983MNRAS.202..657C

(basically as applied to Cir X-1 by Murdin *et al.* 1980). However, there are two serious difficulties with this variant of the model.

(i) Although large N_x values have been deduced in A0538 – 66 (Skinner 1981) there is no regular 16.6 day modulation in the spectrum (particularly in the early observations by White & Carpenter (1978) as noted by Murdin *et al.*)

(ii) It is hard to account for the simultaneous X-ray and optical outburst if the X-rays are 'on' at apastron and 'off' at periastron.

We now turn to the process which we believe must provide the basic source of material in A0538 – 66.

4.1.2 Tidal lobe overflow

The basis of this process is that the neutron star approaches sufficiently close to the primary at periastron that matter is tidally lifted off the primary. This time dependent tidal or Roche lobe overflow is capable of producting large max–min ratios since, at apastron, any material is provided solely by the stellar wind.

4.1.2.1 Estimate of orbital eccentricity. If we assume tidal lobe overflow at periastron with no rotation an eccentricity $e_T = 0.77$ is required.

However, our spectroscopic results (see Table 3) show resolved normal stellar lines at quiescence which we interpret as due to rotation of the primary (and we will take $i \triangleq 0°$) with velocities $\sim 300\,\mathrm{km\,s^{-1}}$. In an eccentric system, we should thus consider the rotational velocities as seen by each component at periastron. Here the neutron star has $v_x = 540\,\mathrm{km\,s^{-1}}$ (for $e = 0.77$) at a separation of 1.04×10^7 km and so, for the primary to have the same instantaneous angular velocity, requires an equatorial velocity of $\sim 400\,\mathrm{km\,s^{-1}}$, which is very close to the observed linewidths (at quiescence). Thus we are justified in using the Roche lobe formulae (Paczynski 1971) appropriate for our mass ratio ($M_x/M_1 = 1/12$) which gives $R_L/D = 0.60$. If the B star *fills* its Roche lobe at periastron then $R_L = R_1$, $D = 1.33 \times 10^7$ km and $e_R = 0.70$.

4.1.2.2 Estimate of mass transfer rate. In Fig. 13(a) we show schematically the periastron passage. Let the primary fill its Roche lobe when the neutron star reaches point B, so that at periastron (point A) L_1 will be below the surface of the primary. For this order of magnitude calculation we will let point B be defined through the angle θ and set 2θ as the

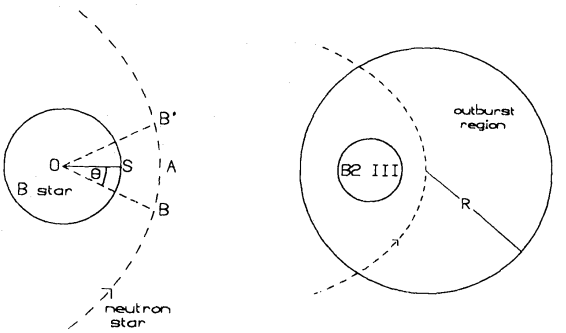

Figure 13. (a) Schematic of periastron passage for the tidal lobe overflow model. θ is set by the typical X-ray outburst time-scale (assumed to represent the mass transfer time-scale). We assume that the primary fills the Roche lobe at B and hence L_1 is below the primary's surface at A. (b) Relative sizes of the emitting regions. This is scaled for a B2 III primary of $R_1 = 11.5\,R_\odot$ and an outburst emission region of $45\,R_\odot$ obtained from the *IUE* continuum fits.

Downloaded from http://academic.oup.com/mnras/article-abstract/202/3/657/967884
by Dartmouth College Library user
on 26 April 2018
© Royal Astronomical Society • Provided by the NASA Astrophysics Data System

1983MNRAS.202..657C

interaction time which will be ~ X-ray outburst time-scale (say 8 hr ~ $P/50$). Considering the neutron star to move (at periastron) at a constant 440 km s^{-1} (using $e_R = 0.70$) then $\theta = 25°$. The separation at B is 1.4×10^7 km and so the primary's radius is 8.43×10^6 km (i.e. the Roche radius). By the time the neutron star reaches periastron (a separation of 1.35×10^7 km) the Roche radius will be 8.10×10^6 km which is a volume approximately 2.8×10^{35} cm^3 less than at point B. If we assume an outer stellar atmosphere of density ~ 10^{-9} g cm^{-3} (Allen 1973) then ~ 2.8×10^{26} g (or $1.4 \times 10^{-7} M_\odot$) could be *available* for mass transfer. Since this is spread over the 8 hr interaction time it corresponds to a potential mass transfer rate ~ $1.5 \times 10^{-4} M_\odot$ yr^{-1}, and an efficiency of ~ 10^{-3} would be sufficient to power the outburst at the observed luminosity.

4.1.2.3 Size of the outburst region. A simple geometrical calculation of the X-ray heating effect on the primary at periastron gives

$$L_{\text{opt}} \triangleq \frac{\alpha}{4}\left(\frac{R_1}{D}\right)^2 L_x \sim 0.05 L_x$$

if we take the X-ray albedo, $\alpha \sim 0.5$. Thus X-ray heating alone should produce an optical flux ~ 5×10^{37} erg s^{-1} at maximum, an effect much greater than in any other early-type X-ray binary. However, the process must be much more complex than this because:

(1) in other X-ray binaries where X-ray heating is an important effect (e.g. Cyg X-2, Her X-1) the resulting optical flux becomes *more* ultraviolet, whereas in A0538 – 66 (see Table 1 and Fig. 3) the star reddens.

(2) Regardless of the actual process the optical flux must come from a region at least the size of the equivalent blackbody radiator. This latter point may be quantified with reference to the fits of model stellar atmospheres to the *IUE* quiescent and outburst spectra given in Section 3.2 which indicate an increase in size from ~ $12 R_\odot$ to ~ $45 R_\odot$.

Hence this large volume of material could completely surround the neutron star as indicated in Fig. 13(b). This confirms our previous section in that the mass transfer (or expansion) is caused by the passage of the neutron star. This material has to have been taken from the primary or at least left from the previous passage (see e.g. the simulations of Haynes, Lerche & Wright 1980). If this outburst volume given above were uniformly filled by the ~ $1.4 \times 10^{-7} M_\odot$ estimated in the last section it would give $n_H \sim 10^{12}$ cm^{-3} and a line-of-sight column density ~ 4×10^{24} cm^{-2}. This calculation is approximate because the large X-ray luminosity will ionize an appreciable fraction of this volume and hence make it more transparent to X-rays. Nevertheless this column density is only slightly higher than that observed during an outburst by Skinner (1981) of $N_x \gtrsim 2.10^{23}$ cm^{-2}.

Tidal dissipation in the periodically expanded envelope will also contribute to the optical outburst. We estimate the energy available as ~ $GM_1 \Delta M/R$, where ΔM is the envelope mass. If we take $\Delta M \sim 10^{-7} M_\odot$ the tidal energy dissipated is ~ 10^{41} erg and the contribution to the luminosity is ~ 10^{36} erg s^{-1} (spread over the interaction time). This is insufficient to power the optical outburst, but still a significant effect.

Pakull & Parmar (1981) also infer an eccentric binary system for A0538 – 66 with discrete mass transfer due to passage of the compact object (at periastron) through a disc-like stellar ring (not in the orbital plane) about a rapidly rotating B star. This model has severe problems, including (1) theoretical difficulties in maintaining the integrity of a disc about the *primary* in an eccentric system; and (2) as shown above the size of the outburst region will almost certainly disrupt any ring, whose regeneration will take ~ years (see e.g. Slettebak 1981).

Downloaded from https://academic.oup.com/mnras/article-abstract/202/3/657/967884
by Dartmouth College Library user
on 26 April 2018

© Royal Astronomical Society • Provided by the NASA Astrophysics Data System

1983MNRAS.202..657C

4.2 EVOLUTIONARY STATUS

The location of A0538 – 66 in the star cluster NGC 2034 and its presumed association with that cluster implies an age for A0538 – 66 of $5–8 \times 10^6$ yr (Pakull & Parmar 1981). Although very short this is consistent with the $\sim 8.6 \times 10^6$ yr needed to form a Be/X-ray system in the evolutionary scheme of Rappaport & van den Heuvel (1981). In fact, given the potentially large mass-loss rate, inferred above, it is likely that the X-ray system was only recently formed since these rates cannot have been maintained for $\gtrsim 10^5$ yr (even allowing for the occasional periods of inactivity, such as observed by Pakull & Parmar) and we have observed *no* similar systems in our Galaxy. We would also expect circularization of the orbit on time-scales $\sim 10^5$ yr.

5 Conclusions

The eccentric binary model of A0538 – 66 presented here, in which the neutron star is effectively imbedded in the primary's extended atmosphere at periastron, accounts for the large 16.6 day X-ray modulation. We suggest that X-ray emission outside periastron is due to accretion from gravitationally bound gas, perhaps in the form of a disc around the compact object obtained during the previous periastron passage. Thus some of the difficulties of super Eddington accretion might be alleviated since it is only emitting for a small fraction of each cycle and is never steady. The most recent observations (Section 2.3) indicate that it is possible for this system to remain near optical maximum well after phase 0, although this does seem to be a rare phenomenon. This could be related to the differing lengths of X-ray flares (see Skinner *et al.* 1980), although whether long optical outbursts always accompany long X-ray outbursts remains to be seen.

Considerable support for our proposed model has been given by the discovery of 69 ms X-ray pulsations during outburst (Skinner *et al.* 1982) where the $\dot{P}/P$ is consistent with our $e \sim 0.7$. There remain many theoretical and observational questions including the following.

(1) What is the precise mechanism and dynamics of the mass transfer at periastron?

(2) Is any material accreted at periastron or does it all 'chase' after the receding neutron star?

(3) Is X-ray and optical maximum at periastron or shortly thereafter?

(4) Is this system a very young X-ray source in a short-lived phase (to explain the paucity of such sources) and what type of source will it evolve into?

(5) How can such an eccentric, interacting binary actually be produced? (Is there any evidence for a past episode of explosive mass loss, or supernova event, McCluskey & Kondo 1970).

(6) Long-term study of the time-scales and other characteristics of the extended periods of inactivity will give unique information on the thermal and dynamical relaxation of the B star envelope following enforced mass removal.

If our outline model is correct, A0538 – 66 provides a remarkable opportunity for studying transient X-ray source phenomena and accretion powered stellar eruptions.

Acknowledgments

We are particularly grateful to Jack Baldwin, Mark Phillips and Roberto Terlevich for obtaining spectra for us, to Frank Freeman, Dave Carter and Mark Phillips for assistance at the AAT and to John Hutchings for sending details of his A0538 – 66 spectra. We acknowledge useful discussions with Paul Murdin and Arvind Parmar. We are grateful to MSSSO for 1-m telescope time, PATT and AAT for observing time and the SERC for travel support. LB and RHD acknowledge receipt of SERC studentships and LB an ICI studentship.

Downloaded from http://academic.oup.com/mnras/article-abstract/202/3/657/967984
by Dartmouth College Library user
on 26 April 2018

© Royal Astronomical Society • Provided by the NASA Astrophysics Data System

1983MNRAS.202..657C

References

Abbott, D. C., Bieging, J. H. & Churchwell, E., 1981. *Astrophys. J.,* **250,** 645.

Allen, C. W., 1973. *Astrophysical Quantities,* 3rd edn, Athlone, London.

Avni, Y. & Goldman, I., 1980. *Astr. Astrophys.,* **90,** 44.

Barlow, M. J., 1982. *IAU Symp. 99,* in press.

Barlow, M. J. & Cohen, M., 1977. *Astrophys. J.,* **213,** 737.

Bath, G. T., Pringle, J. E. & Whelan, J. A. J., 1980. *Mon. Not. R. astr. Soc.,* **190,** 186.

Bohlin, R. C., Holm, A. V., Savage, B. D., Snijders, M. A. J. & Sparks, W. M., 1980. *Astr. Astrophys.,* **85,** 1.

Castor, J. I., Abbott, D. C. & Klein, R. I., 1975. *Astrophys. J.,* **195,** 157.

Castor, J. I., Lutz, J. H. & Seaton, M. J., 1981. *Mon. Not. R. astr. Soc.,* **194,** 547.

Charles, P. A. Booth, L., Densham, R. H., Thorstensen, J. R. & Willis, A. J., 1981. *Space Sci. Rev.,* **30,** 423.

Charles, P. A. & Thorstensen, J. R., 1981. *IAU Circ. 3570.*

Clayton, G. & Thompson, I., 1981. *IAU Circ. 3590.*

Dachs, J. A., 1972. *Astr. Astrophys.,* **18,** 271.

Davidson, K. & Ostriker, J., 1973. *Astrophys. J.,* **179,** 585.

Giddings, J. R., 1981. *IUE/ESA Newsletter,* **12,** 22.

Gursky, H., Dupree, A. K., Hartmann, W., Raymond, J., Davis, R. J., Black, J., Matilsky, T. A., Howarth, I. D., Willis, A. J., Wilson, R., Sandford, M. C. W., Vanden Bout, P., Sanner, F., Hammerschlag-Hensberge, G., van den Heuvel, E. P. J., Lamers, H. J. G. L. M., Burger, M. & de Loore, C., 1980. *Astrophys. J.,* **237,** 163.

Hammerschlag-Hensberge, G., 1980. *Proc. Symp: The 2nd European IUE Conf.,* eds Battrick, B. & Mort, J., *ESA Spec. Pub.. 157.*

Haynes, R. F., Lerche, I. & Wright, A. E., 1980. *Astr. Astrophys.,* **81,** 83.

Hutchings, J. B., 1976. *Be and Shell Stars, IAU Symp. No. 70,* p. 13.

Hutchings, J. B., Cowley, A. P. & Crampton, D., 1981. *IAU Circ. 3585.*

Johnston, M. D., Griffiths, R. E. & Ward, M. J., 1980. *Nature,* **285,** 26.

Kriss, G. A., Rappaport, S., Remillard, R. A., Cominsky, L. R., Williams, G. & Thorstensen, J. R., 1982. Preprint.

Lamers, H. J., 1980. *The Universe in the Ultraviolet, Proc. Symp:* ed. Chapman, R. D., *NASA Conf. Pub., 2171,* p. 93.

Lamers, H. J. G. L. M., 1981. *Astrophys. J.,* **245,** 593.

Long, K., Helfand, D. J. & Grabelsky, D. A., 1981. *Astrophys. J.,* **248,** 925.

Margon, B., Nelson, J., Chanan, G., Thorstensen, J. R. & Bowyer, S., 1977. *Astrophys. J.,* **216,** 811.

McClintock, J. E., Canizares, C. R. & Tarter, B. C., 1975. *Astrophys. J.,* **198,** 641.

McClusky, G. E. & Kondo, Y., 1970. *Astrophys. Space Sci.,* **10,** 464.

Murdin, P., Branduardi-Raymont, G. & Parmar, A., 1981. *Mon. Not. R. astr. Soc.,* **196,** 95P.

Murdin, P., Jauncey, D. L., Haynes, R. F., Lerche, I., Nicolson, G. D., Holt, S. S. & Kaluzienski, L. J., 1980. *Astr. Astrophys.,* **87,** 292.

Nandy, K., Thompson, G. I., Jamar, C., Monfils, A. & Wilson, R., 1976. *Astr. Astrophys.,* **51,** 63.

Oke, J. B. & Schild, R. E., 1970. *Astrophys. J.,* **161,** 1015.

Paczynski, B., 1971. *A. Rev. Astr. Astrophys.,* **9,** 183.

Pakull, M. & Parmar, A., 1981. *Astr. Astrophys.,* **102,** L1.

Panagia, N., 1973. *Astr. J.,* **78,** 929.

Rappaport, S. & van den Heuvel, E. P. J., 1981. *Be Stars, IAU Symp. No. 98,* p. 327.

Seaton, M. J., 1979. *Mon. Not. R. astr. Soc.,* **187,** 73P.

Skinner, G. K., 1980. *Nature,* **288,** 141.

Skinner, G. K., 1981. *Space Sci. Rev.,* **30,** 441.

Skinner, G. K., Shulman, S., Share, G., Evans, W. D., McNutt, D., Meekins, J., Smathers, J., Wood, K., Yentis, D., Byram, E. T., Chubb, T. A. & Friedman, H., 1980. *Astrophys. J.,* **240,** 619.

Skinner, G. K., Leahy, D., Elsner, R. F., Weisskopf, M. C. & Grindlay, J. E., 1982. *IAU Circ. 3671.*

Slettebak, A., 1981. *Be Stars, IAU Symp. No. 98,* p. 109.

Snijders, M. A. J., 1980. *SRC IUE Newsletter.*

Thorstensen, J. R., Charles, P. A. & Bowyer, S., 1978. *Astrophys. J.,* **220,** L131.

White, N. E. & Carpenter, G. F., 1978. *Mon. Not. R. astr. Soc.,* **183,** 11P.

Willis, A. J., Wilson, R., Vanden Bout, P., Sanner, F., Black, J., Davis, R. J., Dupree, A. K., Gursky, H., Hartmann, L., Raymond, J., Matilsky, T., Burger, M., de Loore, C., van Dessel, E. L., Whiteoak, P., Menzies, J., Meikle, W. P. S., Joseph, R. D., Sanford, P., Pollard, G. & Sandford, M. C. W., 1980. *Astrophys. J.,* **237,** 596.

Yamashita, Y., Nariai, K. & Norimoto, Y., 1977. *An Atlas of Representative Stellar Spectra,* University of Tokyo Press.

Downloaded from https://academic.oup.com/mnras/article-abstract/202/3/657/967884
by Dartmouth College Library user
on 26 April 2018

© Royal Astronomical Society • Provided by the NASA Astrophysics Data System